Exploring the extent to which shared mechanisms contribute to motion-position illusions

Timothy V. Cottier Melbourne School of Psychological Sciences, the University of Melbourne, Melbourne, Australia

William Turner Melbourne School of Psychological Sciences, the University of Melbourne, Melbourne, Australia
School of Psychology and Counselling, Queensland University of Technology, Brisbane, Australia

Alex O. Holcombe School of Psychology, the University of Sydney, Sydney, Australia

Hinze Hogendoorn Melbourne School of Psychological Sciences, the University of Melbourne, Melbourne, Australia
School of Psychology and Counselling, Queensland University of Technology, Brisbane, Australia

Motion-position illusions (MPIs) are visual motion illusions in which motion signals bias the perceived position of an object. Due to phenomenological similarities between these illusions, previous research has assumed that some are caused by common mechanisms. However, this assumption has yet to be directly tested. This study investigates this assumption by exploiting between-participant variations in illusion magnitude. During two sessions, 106 participants viewed the flash-lag effect, luminance flash-lag effect, Fröhlich effect, flash-drag effect, flash-grab effect, motion-induced position shift, twinkle-goes effect, and the flash-jump effect. For each effect, the magnitude of the illusion was reliable within participants, strongly correlating between sessions. When the pairwise correlations of averaged illusions magnitudes were explored, two clusters of statistically significant positively correlated illusions were identified. The first cluster comprised the flash-grab effect, motion-induced position shift, and twinkle-goes effect. The second cluster comprised the Fröhlich and flash-drag effect. The fact that within each of these two clusters, individual differences in illusion magnitude were correlated suggests that these clusters may reflect shared underlying mechanisms. An exploratory factor analysis provided additional evidence that these correlated clusters shared an underlying factor, with each cluster loading onto their own factor. Overall, our results reveal that, contrary to the prevailing perspective in the literature, while some motion-position illusions share processes, most of these illusions are unlikely to reflect any shared processes, instead implicating unique mechanisms.

Introduction

Motion-position illusions (MPIs) broadly refer to a class of visual illusions in which the position of an object in the context of motion is incorrectly perceived. Illusions from this class (e.g., the flash-lag effect) have been extensively studied over the past several decades, with the possible underlying mechanisms hotly debated (Eagleman & Sejnowski, 2007; Hogendoorn, 2020; Hubbard, 2014; Krekelberg & Lappe, 2001; Nijhawan, 2008; Schneider, 2018). Despite the phenomenological similarities between MPIs, few published empirical studies have empirically explored their underlying factorial structure (i.e., do they share mechanisms or not). Consequently, little is known about the degree to which these qualitatively similar illusions (and their variations) share underlying neural mechanisms. On the one hand, conceptual similarities between some of these effects have led some authors to argue for a common underlying cause (e.g., Eagleman & Sejnowski, 2007; Schneider, 2018). On the other hand, more recent results suggest that at least some MPIs can best be explained by an interplay of multiple idiosyncratic mechanisms (e.g., Blom et al., 2019; Takao et al., 2022), challenging

Citation: Cottier, T. V., Turner, W., Holcombe, A. O., & Hogendoorn, H. (2023). Exploring the extent to which shared mechanisms contribute to motion-position illusions. *Journal of Vision*, *23*(10):8, 1–24, https://doi.org/10.1167/jov.23.10.8.

https://doi.org/10.1167/jov.23.10.8 Received June 9, 2023; published September 13, 2023 ISSN 1534-7362

the idea that these illusions are manifestations of the same neural processes. It therefore remains unclear to what extent MPIs are caused by shared or dissociable mechanisms.

To investigate this, we concurrently investigate eight different MPIs (Figure 1), using between-subjects variations in illusion magnitude to evaluate which of these illusions are likely to share underlying mechanisms. Specifically, we investigate (A) the flash-lag effect (Nijhawan, 1994), (B) the luminance flash-lag effect (Sheth et al., 2000), (C) the Fröhlich effect (Fröhlich, 1924), (D) the flash-drag effect (Whitney &

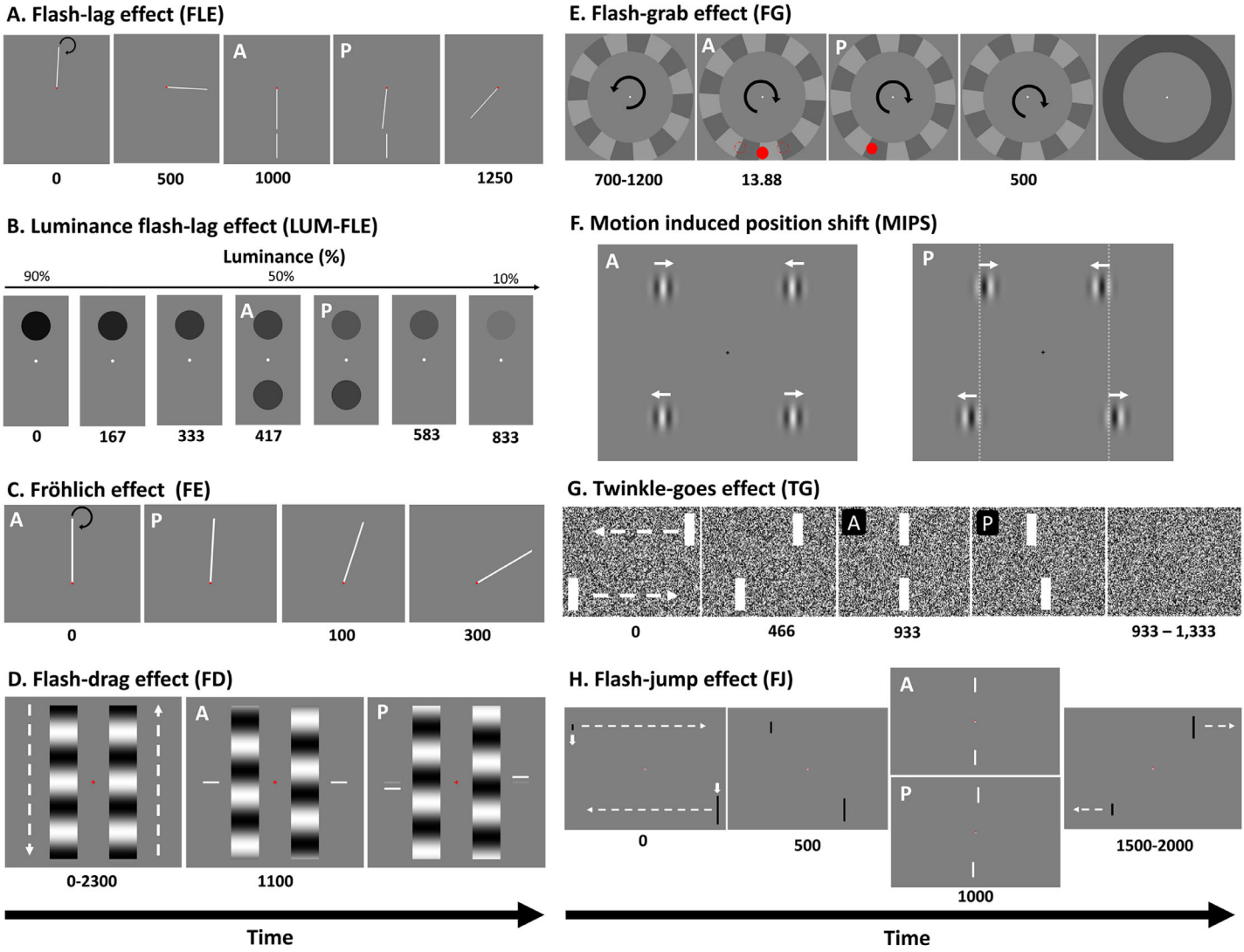

Figure 1. Experimental paradigms. Stylized depictions of example trials for the eight motion-position illusions used in this study. Video examples for each illusion can be accessed at https://tcottier96.github.io. For all images, panels marked as "A" indicate the actual position of the object, and "P" indicates the perceived position of the object. (**A**) Flash-lag effect (FLE): a rod rotates clockwise around the fixation point for 1,250 ms. After 1 second, a stationary rod is briefly flashed in spatiotemporal alignment with the moving rod (actual). However, the moving rod is perceived mislocalized along its clockwise trajectory (perceived). (**B**) Luminance flash-lag effect (LUM-FLE): the top circle decreases in luminance over 833 ms. Halfway through the trial, on the opposite side of the fixation point, a circle with identical instantaneous luminance is briefly presented (actual). Even though both circles have identical luminance values, the target circle is perceived further along its luminance trajectory and thus is perceived to be brighter than the flashed circle (perceived). (**C**) Fröhlich effect (FE): a rod rotates clockwise around the fixation point. When the rod initially appears, it is pointing straight up (actual), but it will be perceived in a position along its clockwise trajectory (perceived). (**D**) Flash-drag (FD) effect: two

→

←
sinusoidal gratings move in opposite directions for 2,300 ms. In this trial, the right grating is moving upward, while the left grating moves downward. After 1,100 ms, two bars are flashed on the outside of each grating. While these bars are presented in vertical alignment (actual), they are perceived mislocalized in the direction of their nearest grating's motion (perceived). (**E**) Flash-grab effect (FG): an annulus rotates counterclockwise for 800 ms, then reverses direction and rotates counterclockwise for 500 ms before turning gray. At the moment the annulus reverses direction, a red circle is flashed for 13.88 ms in one of three positions (the dotted red lines). After the annulus turns gray, participants report the perceived location of the target with a mouse click. In this trial, the red circle was presented at the bottom center of the annulus (actual). However, this circle is perceived to be displaced in the reversal's direction of motion (perceived). (**F**) Motion-induced position shift (MIPS): two pairs of vertically aligned gratings are presented (actual). The phase of the top gratings drifts toward the fixation point, while the phase of the bottom gratings drifts away from the fixation point. Even though the gratings are vertically aligned, they are perceived offset in their direction of motion (perceived). (**G**) Twinkle-goes effect (TG): two bars translate toward one another for 933 ms. The top bar is moving right to left, and the bottom bar is moving left to right. When the bars are vertically aligned (actual), they disappear on a background of dynamic noise. The perceived offset positions of the two bars are shifted forward along their respective trajectories, such that they are seen as misaligned (perceived). (**H**) Flash-jump effect (FJ): involves two bars moving toward each other and changing in height. In this trial, the top bar was moving right to left and increasing in height, while the bottom bar moved left to right while decreasing in height. When the two bars reach the center of the screen and are physically aligned, they will be the same height and briefly become white (actual). This brief color change is mislocalized further along the motion and growth trajectory of the bar and as such is perceived when the bar is a different size and not vertically aligned with the other bar (perceived).

Cavanagh, 2000), (E) the flash-grab effect (Cavanagh & Anstis, 2013), (F) the motion-induced position shift (De Valois & De Valois, 1991; Ramachandran & Anstis, 1990), (G) the twinkle-goes effect (Nakayama & Holcombe, 2021), and the (H) the flash-jump effect (Cai & Schlag, 2001). First, we begin by briefly reviewing each of these illusions.

Flash-lag effect

The flash-lag effect (FLE) is the most-studied MPI. In the FLE, a stationary rod briefly presented in spatiotemporal alignment with a continuously rotating rod is perceived in a position behind the rotating rod (Nijhawan, 1994). It was originally observed by Metzger (1932) and subsequently rediscovered by Mackay (1958) before its popularity exploded when Nijhawan (1994) reported it as evidence for motion extrapolation. Nijhawan's proposal that the illusion results from motion extrapolation has been hotly contested over the past three decades, with numerous alternative mechanisms having been proposed (for reviews, see Hogendoorn, 2020; Hubbard, 2014; Krekelberg & Lappe, 2001; Nijhawan, 2008). These include postdiction (Eagleman & Sejnowski, 2000), temporal integration (Krekelberg & Lappe, 2000, 2001), attentional shifting (Baldo & Klein, 1995), differential latencies (Whitney et al., 2000; Whitney & Murakami, 1998), representational momentum (Hubbard, 2014), and, most recently, discrete sampling (Schneider, 2018). Some authors have argued that these mechanisms can explain not just the FLE but other MPIs (Eagleman & Sejnowski, 2007; Schneider, 2018). If this were true, we would expect to observe strong positive correlations between the FLE and other paradigms.

Luminance flash-lag effect

The FLE is not unique to motion perception and has been reported in other feature spaces, including luminance, spatial frequency, entropy, and color (Sheth et al., 2000). In these variants, one target object continuously changes on a particular feature dimension (e.g., luminance), and a second object with identical features is briefly flashed alongside the target. The flash is perceived to lag the target on the changing feature. For example, in the luminance flash-lag effect (LUM-FLE), a target circle is smoothly changing in luminance (e.g., becoming brighter). A second circle is flashed on the opposite side of fixation with identical instantaneous luminance as the target circle. However, participants will not perceive the two circles to have the same luminance, instead perceiving the target circle further along its luminance trajectory (i.e., brighter than the flash).

Fröhlich effect

The Fröhlich effect (FE) is the illusory effect that when a moving object first appears, its onset position is not perceived in its true position but is instead perceived in a position further along its motion trajectory (Fröhlich, 1924; Hubbard, 2014). The phenomenological similarity between the Fröhlich and flash-lag effects has led to suggestions that both are manifestations of the same underlying neural processes (Eagleman & Sejnowski, 2007; Hubbard, 2014). However, this suggestion was not supported by the findings of a recent individual differences study (Morrow & Samaha, 2022).

Flash-drag effect

The flash-drag effect (FD) is the phenomenon that the perceived position of a stationary object briefly presented adjacent to a moving object is dragged in the direction of the moving object's motion (Whitney & Cavanagh, 2000). The magnitude of this effect is generally smaller than the FLE, and Eagleman and Sejnowski (2007) note that in most experimental paradigms, the FD and FLE should operate in opposite directions. This is because the FD can cause the flash in the FLE to be dragged in the direction of motion, such that the "true" FLE is underestimated. If this is true, variations in FD magnitude across observers might be expected to negatively correlate with FLE magnitude.

Flash-grab effect

In the flash-grab effect (FG), a static object is briefly flashed on a moving texture as the texture abruptly changes direction. The result is that the perceived position of the flashed object is shifted in the texture's new direction of motion (Blom et al., 2019; Cavanagh & Anstis, 2013). Although similar to the FD, in that it involves a moving texture, there are some important differences. First, the magnitude of the FG is substantially larger than the FD (and most other MPIs; Cavanagh & Anstis, 2013). In addition, the FG is the sum of at least two separate mislocalizations (backward along the preflash motion vector and forward along the postflash motion vector) (Blom et al., 2019). Finally, Takao et al. (2022) found that none of the traditional FLE models (e.g., differential latency, extrapolation, temporal integration) can fully explain the FG, concluding that it is likely produced by two or more processes.

Motion-induced position shift

Stationary envelopes containing internal motion are perceived displaced in the direction of that motion (Anstis, 1989; De Valois & De Valois, 1991; Ramachandran & Anstis, 1990). A powerful demonstration of this effect can be achieved by viewing two Gabor patches drifting in opposite directions within aligned static envelopes, which causes a large apparent misalignment between the two patches (De Valois & De Valois, 1991). Linares and Holcombe (2008) found a dissociation between this illusion and the FLE, in that the motion-induced position shift effect was stronger for motion away from the fovea, while the FLE was greater for motion toward the fovea, suggesting these illusions may involve different mechanisms.

Twinkle-goes effect

The twinkle-goes effect (TG) is the observation that when a moving object disappears concurrently with the presentation of a dynamic noise background, it is perceived to overshoot the point at which it disappears (Nakayama & Holcombe, 2021). The effect does not occur if the moving object disappears on a static noise background. Importantly, this pattern of results directly parallels studies of the FLE, where manipulations that mask the disappearance of the moving object similarly cause overshoots in the perceived disappearance position (Maus & Nijhawan, 2006, 2008; Shi & Nijhawan, 2012), suggesting there may be some overlap in the underlying mechanisms.

Flash-jump effect

In the flash-jump effect (FJ), a transient color change in a moving object is perceived to occur further along the object's trajectory than it physically did. In the original demonstration (Cai & Schlag, 2001), a moving bar gradually changing in height undergoes a brief color change. The location at which this color change occurs is mislocalized further along the bar's trajectory and on a bar of a different height (Cai & Schlag, 2001; Eagleman & Sejnowski, 2007). Schneider (2018) proposed that the FJ could be a variant of the FLE, but this seems unlikely as the perceived position of the transient color change is displaced along the trajectory, rather than lagging behind the object as in the FLE. Instead, the FJ might be argued to be more similar to the FD than the FLE, because it involves a transient feature being displaced along the motion trajectory.

Individual differences in illusion magnitude

Traditionally, visual perception research seeks to characterize a standard observer by identifying the functions of the visual system that are common across humans (Clark et al., 2022; Hedge et al., 2018). As a consequence, differences between observers are often treated as measurement noise to be minimized (Mollon et al., 2017). However, the visual abilities of people do vary greatly (Ward et al., 2017), and this variation often represents "real differences in optical, neural, and cognitive processes that mediate perception" (Mollon et al., 2017, p. 4). For example, Schwarzkopf et al. (2011) reported a negative relationship between the surface area of observers' V1 and the strength of illusory effects in the Ebbinghaus (size context illusion) and Ponzo (parallel) illusions, two geometric illusions where context influences perceived size.

Although the phenomenological similarity between MPIs seems to suggest that the illusions are mechanistically similar, there is yet limited experimental evidence to bolster this assumption. This gap can be addressed by adopting an individual differences approach. This is because individuals will have a similar susceptibility to illusions that are caused by common factors (Grzeczkowski et al., 2017), such that measured illusion magnitudes will correlate highly with one another (Mollon et al., 2017). For example, recent studies using an individual differences approach have revealed that geometric illusions are unlikely to be caused by a single common factor (Grzeczkowski et al., 2017); instead, each illusion may be caused by its own specific factor (Cretenoud et al., 2019). Similarly, Wexler et al. (2022) investigated biases in different motion stimuli and identified both correlated and uncorrelated effects, leading them to suggest that motion perception biases are unlikely to be caused by a single global factor but may instead be caused by dissociable local factors. Using different motion perception paradigms, Hu et al. (2022) similarly observed limited correlations between different motion perception paradigms (motion-induced spatial conflict, motion-induced position shift, the adaptation-induced spatial shift accrual rate, smooth motion threshold).

To date, only one study has used an individual differences approach to study MPIs. Morrow and Samaha (2022) investigated the Fröhlich effect and the FLE using an individual differences approach with 24 participants. They found that individual magnitudes in the two illusions were uncorrelated, suggesting that these illusions are caused by dissociable mechanisms. These findings corroborate observations by Gauch and Kerzel (2008, Experiment 4, $N = 14$) who found a version of the Fröhlich effect and the flash-lag effect were not significantly correlated. However, a limitation of both studies is their small sample sizes, which provide limited statistical power to detect between-subject effects. Additionally, both studies only looked at two MPIs (the FLE and FE). Therefore, the extent to which these or other MPIs recruit dissociable or shared mechanisms remains unknown.

The present study addresses these limitations by characterizing the relationships between eight different MPIs in a larger sample. This allows us to evaluate the extent to which (if any) these illusions share common neural mechanisms. Analysis of the correlations suggests an underlying factorial structure with two clusters of illusions that share a common underlying process. The first cluster comprises the motion-induced position shift (MIPS), the twinkle-goes illusion (TG), and the flash-grab effect (FG), and the second cluster comprises the flash-drag (FD) and Fröhlich effect (FE). The association between the MIPS, TG, and FG, and the FD and FE, was subsequently corroborated by an exploratory factor analysis. Overall, our pattern of results shows that some MPIs share common underlying mechanisms, but despite their phenomenological similarities, and contrary to the prevailing assumption in the field that they are caused by the same mechanisms, many of these phenomena arise from dissociable mechanisms.

Method

Participants

In total, 116 participants were recruited from the University of Melbourne's research participant pool. Participants completed this study for either monetary compensation or course credit in an undergraduate psychology subject. All participants completed two sessions. Ten participants were excluded from the final analysis because they completed the first session but failed to complete a second session. The final sample ($N = 106$) was aged between 18 and 49 years ($M_{age} = 21.05$, $SD_{age} = 4.94$; 78 females). All participants reported having no neurological deficits or disorders and having normal or corrected-to-normal vision. In total, 104 participants reported being primarily right-handed (all participants used their right hand to use the computer mouse). This study was approved by the University of Melbourne's Human Research Ethics committee (ID: 2022-12816-29275-8). All participants provided written informed consent.

Apparatus

The stimuli were presented using PsychoPy (v2021.2.3; Peirce et al., 2019, 2022) on HP EliteDesk 800 G3 TWR desktop PCs with Nvidia GeForce Gtx1060s, running Windows 10 Pro (v.1803; Microsoft, 2018). Stimuli were presented on 24.5-in. ASUS PG258Qs with a resolution of 1,920 × 1,080 pixels and a refresh rate of 144 Hz. Monitors were gamma corrected using a Cambridge Research Systems Colorcal MKII (Cambridge Research Systems, 2018). Participants viewed the stimulus with their head stabilized on a chin and forehead rest approximately 50 cm from the monitor.

Overall procedure

All participants completed two experimental sessions. During each session, each participant completed eight separate experimental blocks—one for each of the eight MPIs that make up this study (Figure 1). Each of the two sessions took between 2 and 2.5 hours to complete and were completed on separate days. On average, the

second session took place 5.2 days (minimum = 1 day, maximum = 21 days) after the first session.

The order of the eight different MPIs was randomized for each participant and for each session. Prior to each experimental block, participants received written and verbal instructions about the task and completed a survey on a separate computer to verify their understanding of task instructions. The experimenter then checked participants' understanding a final time. Finally, participants completed practice trials for all tasks (except the FE due to time constraints) while the experimenter observed. In all experimental blocks, participants completed the task alone in a dark room, with their head stabilized on a chinrest. Participants were asked to maintain fixation on a central fixation point throughout the experiment.

Experimental paradigms

For each observer and each session, the magnitude of the eight MPIs was tested in eight separate experimental blocks. In all tasks, stimuli were presented on a gray background, with a fixation point (subtending approximately 0.3 to 0.5 degrees of visual angle [dva]) in the center of the screen. The dimensions for the different features of each illusion are presented below. Participants completed the same eight tasks in both sessions. Breaks were provided throughout each session, without a time limit. The experiment code is publicly available at https://osf.io/s4aqg/?view_only=a7261cdc610549e9a07141c7fffb9e57.

Flash-lag effect (FLE)

For this study, we created our own version of the flash-lag effect (Nijhawan, 1994). Connected to the fixation point dot was a target rod (8.6 dva long and 0.19 dva wide) that rotated clockwise or counterclockwise around the fixation point at a speed of 180 degrees of polar angle per second. The rod randomly rotated for 1,250 ms, 1,500 ms, 1,750 ms, or 2,000 ms before disappearing, and 250 ms prior to the target's disappearance, a static rod (5.12 dva long and 0.19 dva wide) was briefly flashed for 49 ms. The edge of the flash and target rod were separated by 3.5 dva. The flash was always presented at a radius of 12.15 dva from the fixation dot. The flash was presented an equal number of times in five positions in both the upper and lower visual fields. It was presented at the horizontal meridian, offset 5 degrees of polar angle to the right or left, or offset 15 degrees of polar angle to the right or left. Participants completed 8 practice trials, followed by 160 experimental trials. Throughout the task, participants were instructed to report which of the target or flashed rod was further along the motion trajectory of the moving target rod at the time of the flash. During the practice trials, feedback was provided on whether participants correctly indicated which line was ahead.

The polar angle offset between the flash and the target rod was controlled by four randomly interleaved independent 1-up, 1-down adaptive staircases (40 trials per staircase), with two staircases for each rotation direction of the rod (clockwise or counterclockwise). To avoid hysteresis effects, for each rotation direction, one staircase began with the flash position offset 28 degrees of polar angle in the rod's direction of motion, while the other began with the flash offset 28 degrees in the direction opposite motion. Participants used the keyboard to indicate which line was ahead at the time of the flash. Flash offset was initially adjusted by increments of 4 degrees of polar angle, which reduced to increments of 2 degrees of polar angle after three reversals.

Luminance flash-lag effect (LUM-FLE)

Our luminance variant of the FLE was based on the original paradigm by Sheth et al. (2000). On each trial, on a gray background (143 cd/m^2), a black target circle either above or below the central fixation dot smoothly changed in luminance (0.13 cd/m^2 per ms) for 833 ms. On half of the trials, this circle would increase in luminance (from black to gray) by gradually changing from 22 to 132 cd/m^2. On the other half of trials, the target circle would decrease in luminance from gray (132 cd/m^2) to black (22 cd/m^2). Halfway through the task (416.4 ms), when the target circle had a luminance of 80 cd/m^2, a circle was flashed for 14 ms on the opposite side of the fixation dot to the target. Both circles subtended 2.9 dva, and the center of both circles was at an eccentricity of 3.5 dva from the fixation dot. Participants used the keyboard to report which of the two circles was darker at the moment of the flash, completing 8 practice trials, followed by 240 experimental trials, with a break halfway. During the practice trials, feedback was provided on whether participants correctly indicated which circle was darker.

The contrast of the flashed circle was controlled by four randomly interleaved independent 1-up, 1-down adaptive staircases (60 trials each). To avoid the hysteresis effect, for each luminance change trajectory of the target (darkening vs. lightening), one staircase started with flash luminance contrast at 100% and the other at 10%. Flash luminance contrast was adjusted in 5% increments after each trial.

Fröhlich effect (FE)

This study's Fröhlich effect paradigm was similar to our flash-lag effect paradigm, with the exception that no flash was presented. Connected to the fixation dot was a black rod 10.5 dva long and 0.32 dva wide. This

rod randomly rotated clockwise or counterclockwise around the fixation point at 200 degrees of polar angle per second for 604 ms. Participants completed 160 trials, with a break halfway. The rod's starting position on each trial was controlled by four randomly interleaved independent 1-up, 1-down staircases (40 trials per staircase). For each direction of rod rotation, one staircase began with the rod's position offset 45 degrees of polar angle from vertical in the direction of motion, while the other began with the rod offset from vertical in the opposite direction. Participants used the keyboard to indicate whether the rod was pointing to the left or right of vertical at its onset. The rod's onset position was adjusted after each trial by an increment that changed after every reversal in the staircase direction, from 6 to 3, 2, and finally 1 degree of polar angle.

Flash-drag effect (FD)

Our flash-drag paradigm was based on the original paradigm by Whitney and Cavanagh (2000). Two sinusoidally modulated grayscale linear gratings (20.5 dva high and 3.6 dva wide) with a spatial frequency of 0.15 cycles per dva were presented 3.85 dva to the left and right of a red fixation cross subtending 0.5 dva. In each trial, the two gratings were presented for 2,300 ms, drifting vertically in opposite directions with a speed of 26.7 dva/s. Motion direction reversed after every trial.

During the motion sequence (1,100 ms, 1,400 ms, 1,700 ms, or 2,000 ms after onset), two horizontal white target rectangles (0.25 dva high and 2.05 dva wide) were presented 1.54 dva away from the outer edges of the two gratings for a duration of 56 ms. The vertical positions of the two flashed rectangles were always equally offset from the horizontal midline in opposite directions, with the magnitude of the offset controlled by one of four quasi-randomly presented 1-up, 1-down staircases. For each possible direction of grating motion (up or down), there was one staircase that began with the flash vertically offset 3.52 dva in the direction of motion and one staircase that began vertically presenting the flash 3.52 dva in the direction opposite motion. The presentation of the staircases was quasi-random, in that the staircases were randomly presented in pairs of opposite direction of motion. For example, a staircase with the right grating moving upward would be followed by a staircase with a grating moving downward. All permutations of pairs were explored, such that, for each staircase, it was paired with both staircases for the opposite direction of motion. Participants used a keyboard to report which flash was higher. The four staircases controlled the vertical positions of the two flashes to converge on the point of perceived equality, initially adjusting the flash's vertical position by 0.44 dva, then reducing to 0.22 dva after four staircase reversals. Participants completed 4 practice trials and 208 experimental trials, with a break provided halfway. Throughout the task, participants were asked to report which flash was higher, and during the practice trials, feedback was provided to participants on whether they were correctly indicating the higher flash.

Flash-grab effect (FG)

Our flash-grab paradigm was based on the paradigm used by Hogendoorn et al. (2015). A checkerboard-textured black and white annulus with a radius of 17.8 dva randomly rotated clockwise or counterclockwise at 200 dva/s for a duration of 700 ms, 800 ms, 900 ms, 1,000 ms, 1,100 ms, or 1,200 ms, before reversing direction for 500 ms. At the center of the annulus was a stationary white fixation dot subtending 0.5 dva. When the reversal occurred, a red target circle subtending 3.2 dva was flashed for 14 ms. The red target circle was presented an equal number of times at three positions: the bottom center of the annulus, offset 20 degrees of polar angle to the left of center, or offset 20 degrees to the right of center. The center of the red target was presented at a radius of 14.15 dva from the fixation dot (i.e., centered on the width of the annulus). Participants completed 200 experimental trials: 30 trials for each of the six inducer durations and 20 catch trials in which no target was displayed to participants. Once the annulus had completed its movement, it became gray and participants used the mouse to report the perceived location of the red target on the annulus. When participants did not see the target, they reported this by clicking on the fixation point.

Motion-induced position shift

This paradigm was inspired by De Valois and De Valois (1991). At the center of the screen there was a black fixation cross subtending 0.5 dva. There were four vertically oriented Gabor patches, two to the right and two to the left of the fixation cross, offset 9.61 dva above and below the fixation cross. The Gabor patches had a diameter of 6.41 dva with a contrast of 90% and spatial frequency of 0.46 cycles per dva. On each trial, the Gabors' horizontal positions were randomly chosen from one of three possible combinations of positions: (a) the top and bottom were vertically aligned, with all Gabors offset horizontally by 9.71 dva from fixation; (b) the top Gabors were offset horizontally from fixation by 12.16 dva, while the bottom Gabors were offset horizontally by 7.26 dva; and (c) the top Gabors were offset from fixation by 7.26 dva while the bottom Gabors were offset away from fixation by 12.16 dva. The phase of each Gabor drifted horizontally within its static envelope at a speed of 4.3 dva/s, with each Gabor drifting in the opposite direction to its vertical

partner. For example, the upper pair of Gabors could drift outward while the lower pair drifted inward or vice versa. All Gabors continued drifting throughout each trial, and participants used the keyboard to adjust the horizontal position of the two pairs of Gabors such that they were vertically aligned. Participants completed 60 trials, comprising 20 trials for each of the three different starting offsets. Prior to starting the experiment, participants practiced the task (∼usually two to five trials) in front of the researcher.

Twinkle-goes illusion (TG)

Our twinkle-goes paradigm was based on the initial report of the illusion by Nakayama and Holcombe (2021), using the same stimulus parameters as their Experiment 1. Stimuli were presented on a background of visual noise comprising squares (0.26 × 0.26 dva) with random luminance values. Stimuli consisted of two rectangles (2.9 dva wide × 7.7 dva high), presented diagonally above and below fixation, on opposite sides of the screen (left or right) at an initial eccentricity of 7.7 dva. Both rectangles translated horizontally toward the midline at a speed of 18.1 dva/s for a random duration between 800 and 1,000 ms before disappearing. After the rectangles disappeared, the background noise remained on the screen for 400 ms before disappearing, and the screen went gray. On half of the 320 trials (the illusion condition), 80 ms before the rectangles disappeared, the background noise became dynamic by randomly and independently modulating the luminance values of each of the background noise squares. In the remaining trials (the static noise condition), the original static noise pattern was presented. In both conditions, the fixation point disappeared concurrently with the noise background, after which the screen remained gray until a key response was made.

On each trial, the disappearance location of the squares was controlled by one of eight randomly interleaved adaptive 1-up, 1-down staircases (40 trials per staircase). There were four staircases for each noise condition, two for each direction of motion (left to right or right to left). All staircases began with the squares disappearing out of vertical alignment, offset horizontally either 4.52 dva in the direction of motion or in the opposite direction. Staircases were used to converge on the point of perceived equality, adjusting the displacement between the squares with increments of 0.45 dva. Participants completed 332 trials total: 12 practice trials and 320 experimental trials.

Flash-jump effect (FJ)

The flash-jump paradigm was inspired by the original report by Cai and Schlag (2001). The display consisted of a central fixation point and two vertical bars (0.36 dva wide), presented in diagonally opposite visual quadrants. Starting from a horizontal eccentricity of 14.52 dva, the two bars translated horizontally toward fixation at a speed of 14.52 dva/s for 2,000 ms before disappearing. While the bars were moving, one bar grew in height while the other bar shrunk in height, and the height changed at 4.32 degrees/s. On half of the trials, the top bar grew in height while the bottom bar shrunk in height, with the opposite occurring on the other half of trials. Midway through the motion trajectory, while the bars were vertically aligned, both bars briefly flashed white for 14 ms.

The display repeated continuously while participants used a keyboard to adjust the height of one of the two bars, which we will call the target bar, until it was the same perceived height as the other bar at the instant that they both flashed white. The target bar was presented above fixation on half the trials and below fixation on the other half of trials. The identity of the target bar was indicated to the participant by presenting either the top or the bottom half of the fixation point in red throughout the trial. Stimulus presentation continued until participants pressed the "space" key to indicate that they perceived the bars as being equal height when they flashed white.

Participants completed 51 randomly presented experimental trials, of which the first 3 were practice trials, and 3 were attention checks that occurred every 15 trials. For a third of the experimental trials (15), the bar heights were initially set such that the heights of the two bars were equal when they flashed white. On a further third of trials, the target bar height at the moment of the flash was initially set to 1.93 dva taller than the other bar, and in the final third of trials, the target bar height at the moment of the flash was set to 1.93 dva shorter than the other bar. Offline inspection of presentation data files revealed a degree of temporal imprecision in the presentation timing at the time of the flash on a minority of trials. For example, in the condition when we intended on the bars being the same height at the time of the flash, the flash may have not occurred when the bars were the same height. However, the fact that we observed strong illusory effect (Figure 3) with high test reliability (Figure 2) provides confidence that the paradigm nevertheless measured some perceptual effect.

Analysis

The objective of each of the eight experimental blocks in each session was to estimate the magnitude of the associated MPI for that participant. To do so, five MPIs (FLE, LUM-FLE, FE, FD, TG) used adaptive staircases, FG used direct reports, and MIPS and FJ used a method of adjustment.

For paradigms that did not use adaptive staircases (MIPS, FG, and FJ), the magnitude of the illusion

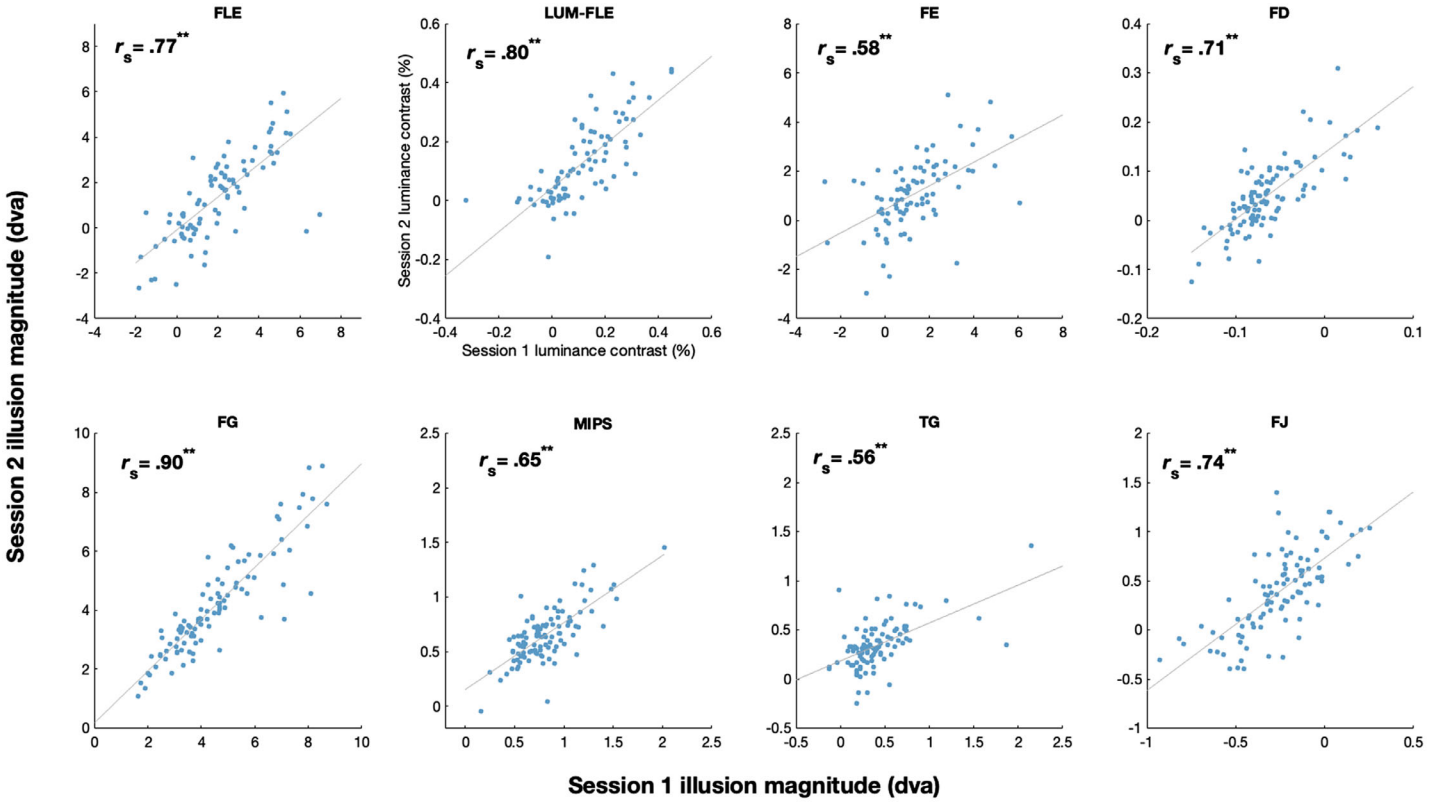

Figure 2. Scatterplots and Spearman's rho correlations between sessions for each MPI (**$p < 0.01$). For all illusions, horizontal and vertical axes show the illusion magnitude in dva (except LUM-FLE, which is in % luminance contrast). Pearson's *r* correlations for these relationships are presented in Table A2.

was simply the mean difference between the reported position and the physical position, in the direction of motion. For illusions with staircases, we calculated the magnitude of the illusion as the averaged difference between the points of subjective equality (PSEs) for each direction of motion of the inducer or target (e.g., clockwise vs. counterclockwise, left vs. right, in the TG–dynamic noise vs. static noise). For the FLE, LUM-FLE, and FD, the PSE for each motion direction was calculated as the average of the final 20 trials of all staircases in that direction (final 10 trials for FE and TG due to fewer available trials).

Illusion-specific details

Flash-lag effect (FLE)

The FLE magnitude was operationalized as the arc length distance in dva between the end of the target rod and the flash, in the direction of motion, averaged across motion directions. In total, 104 participants completed this task. Due to time constraints, two participants did not complete this task during an experimental session. Nineteen participants were excluded from this task's analysis because their staircases did not converge. Staircases were classified as not converged if the difference between the two staircases for a given motion direction (one initialized ahead and one initialized behind) remained greater than 3.18 dva (15 degrees of polar angle). The final sample size for this illusion was 85 participants.

Flash-lag effect luminance (LUM-FLE)

Illusion magnitude was represented as the difference between the PSE of the luminance of the target circle and the flashed circle at the moment of the flash. In total, 105 participants completed this experiment. Due to time constraints, one participant did not complete this task. Twenty-two participants were excluded from this task's analysis because their staircases failed to converge. Staircases were considered not converged if, within any luminance change direction, the difference between the staircases with opposite initial values was greater than 30% luminance contrast. The final sample size for this illusion comprised 83 participants.

Fröhlich effect

FE magnitude was calculated as the arc length difference in dva between the physical starting position of the rod's trailing edge and the vertical midline.

A total of 104 participants completed this task. Two participants did not complete this task in one experimental session because of time constraints. Eight participants were excluded from analysis for this task for pressing the same key in at least 80% of trials in two or more staircases in one session. An additional eight participants were excluded from this illusion's analysis because of their staircases not converging. Staircases were considered not converged if, within a single motion direction, the difference between staircases with opposite starting values remained greater than 8.25 dva (45 degrees of polar angle). The final sample size for this illusion comprised 88 participants.

Flash-drag effect (FD)

FD effect magnitude was operationalized as the vertical distance in dva between the target rectangles and the central fixation point at PSE. A total of 106 participants completed this illusion. One participant did not complete this task during an experimental session because of time constraints. One participant was excluded from this illusion because their staircases failed to converge: Within one direction of motion, the final staircase values differed by more than 3.5 dva. Additionally, another participant's datafile was lost due to an error during saving. The final sample size for this illusion comprised 103 participants.

Flash-grab effect (FG)

FG magnitude on each trial was calculated as the arc length distance in dva between the target's presented position and the participant's reported position. For each reversal direction (clockwise and counterclockwise), a direction-specific effect was calculated by averaging across all trials, and positive errors represented errors in the direction of postreversal motion. A total of 103 participants completed this task in both sessions. Three participants did not complete this task due to time constraints. Four participants were excluded for failing more than 20% of the attention check trials or reporting not seeing the target in more than 10% of the total trials. The final sample size for this illusion comprised 99 participants.

Motion-induced position shift (MIPS)

Illusion magnitude was calculated as half of the average horizontal offset between upper and lower Gabors at the point that observers reported the two to be horizontally aligned. A total of 104 participants completed this task, and no participants were excluded from the analysis. Two participants did not complete this task during an experimental session due to time constraints. Trials in which participants reported an effect with an absolute magnitude of 10 dva or greater were removed as outliers. Six participants had an effect greater than 10 dva but only for a single trial. The final sample size for this illusion comprised 104 participants.

Twinkle-goes

TG magnitude was operationalized as the difference (in dva) between the PSE in trials with dynamic noise and trials with static noise. For each condition, the PSE reflects half the mean horizontal offset from physical vertical alignment at the point of perceptual alignment. A total of 104 participants completed this task. Two participants did not complete this task during an experimental session due to time constraints. Eight participants were excluded because staircases within at least one motion direction did not converge. Within each direction of motion, staircases were considered not converged if staircases with opposite initial values had PSE differences greater than 1.48 dva. The final sample size for this illusion comprised 96 participants.

Flash-jump effect

FJ magnitude was operationalized as half the average difference between the height of the target bar and the reference bar at the moment of the flash in the shrinking versus growing configurations. Illusory effects in the direction of size change (i.e., overestimation of the height for a growing bar) were taken as positive. A total of 103 participants completed this task. Three participants did not complete this task during an experimental session due to time constraints. Six participants were excluded for failing all three attention checks. To eliminate accidental premature responses, trials were considered outliers and excluded from the effect calculation if the magnitude reported on that trial differed by more than 3 *SD*s from that participant's mean effect magnitude. One participant had two trials that were outliers, and 20 participants had one trial that was an outlier. The final sample size for this illusion comprised 97 participants.

Results

To assess the degree of overlap in shared mechanisms underlying the eight different MPIs, we explored the relationships between illusions by correlating illusion magnitude between individuals and conducting an exploratory factor analysis. All statistical analyses were conducted with MATLAB (v.R2021B; The MathWorks Inc., 2021). The analysis code will be made publicly available upon publication at https://osf.io/s4aqg/?view_only=a7261cdc610549e9a07141c7fffb9e57.

Scatterplots showed that for the FE, some participants were outliers with scores above 10 dva or below −10 dva. It is highly unlikely these scores

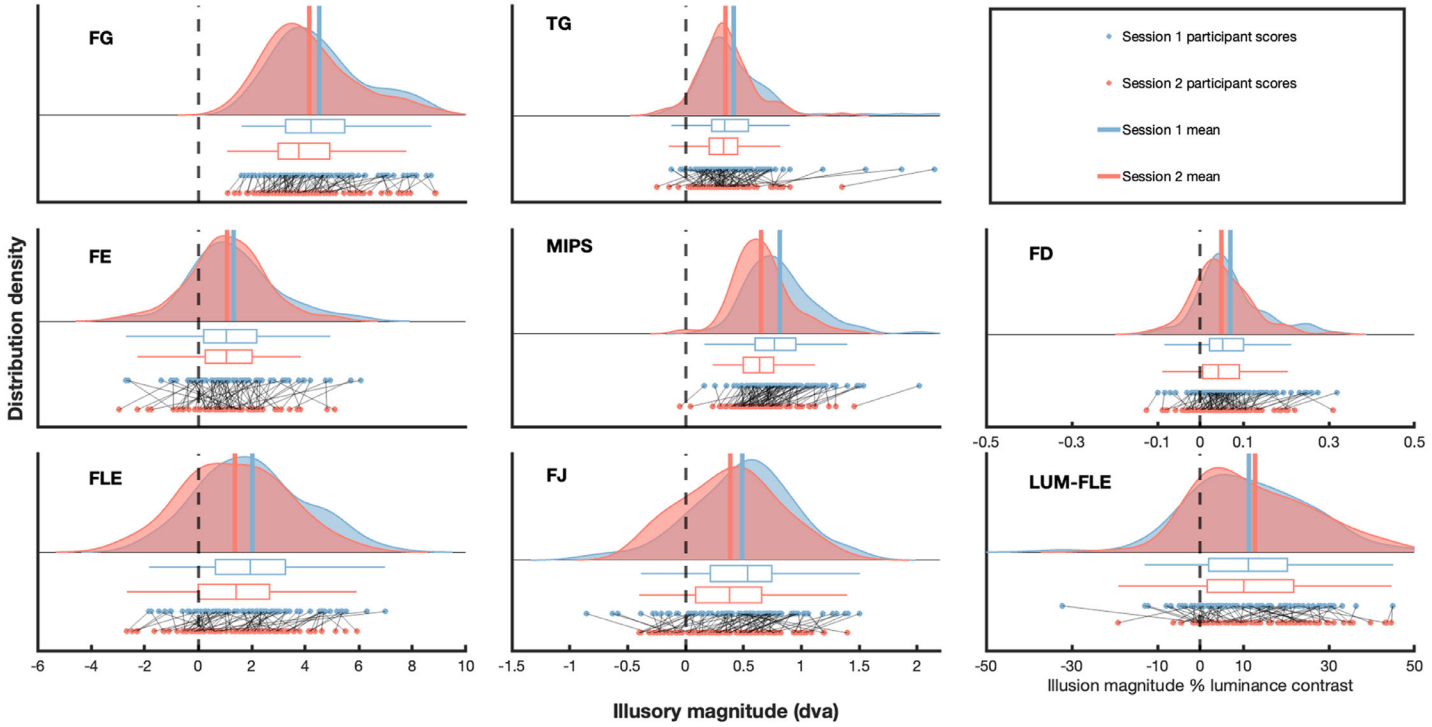

Figure 3. Distribution of individual illusion magnitudes for all eight MPIs. For each illusion, Session 1 is depicted in blue and Session 2 is red. The abscissa's units are degrees of visual angle, except for LUM-FLE, where the unit is luminance contrast (%). The axis ranges are different for each column to accommodate differences in mean size and variability. The dashed black line represents the point corresponding to no illusory effect, with positive values indicating effects in the expected direction. Boxplots show interquartile range, median, maximum, and minimum for each session. The distributions show an estimated probability density distribution created using MATLAB's ksdensity function. Lines connect individual participants' scores for each session.

reflect genuine effects, instead likely representing a misunderstanding of the task instructions. As such, six outliers were removed from this illusion's analysis. Additionally, histograms of illusion magnitudes for each of the eight MPIs were inspected, and it was observed that illusion magnitude variables were nonnormally distributed for both sessions. This was confirmed by significant Kolmogorov–Smirnov tests for each illusion at both session time points (all $p < 0.001$; Table A1). Therefore, nonparametric correlation analyses and bias-corrected and accelerated (Efron & Tibshriani, 1994) 95% bootstrapped confidence intervals ($N = 1{,}000$) are reported and interpreted for all analyses.

Before analyzing correlations between illusion magnitudes across different MPIs, we investigated the test–retest reliability of each illusion. To do so, within each MPI, we examined the correlation in illusion magnitude between Session 1 and Session 2. Overall, reliability was high (intersession Spearman's rho ranged from 0.56 to 0.90; Figure 2), indicating that illusion magnitudes are highly stable across time and validating their use as a between-subjects correlation measure. Having established the reliability of these measurements, we averaged across both sessions to establish a single magnitude measure for each illusion and for each participant.

Descriptive statistics

For each illusion, the distribution of participants' illusion magnitudes and interquartile range, median, mean, and individual scores for each session are presented in Figure 3. Means and standard deviations are provided in Table A3. Raincloud plots were created using the MATLAB function by Allen et al. (2019). We observed strong, reliable illusion effects in all eight MPI paradigms. Qualitatively, FG, TG, and MIPS appear to have the strongest illusory effects, with nearly all individual participants experiencing an illusory effect in the expected direction. In absolute terms, the largest average illusion magnitude was observed in the FG, consistent with previous reports of this illusion being especially strong (Cavanagh & Anstis, 2013).

As shown in Table A3 and Figure 3, for all illusions except the LUM-FLE, there was a reduction in mean illusory magnitude from Session 1 to 2. We were interested in exploring whether this reduction in illusory magnitude was related to the number of days between

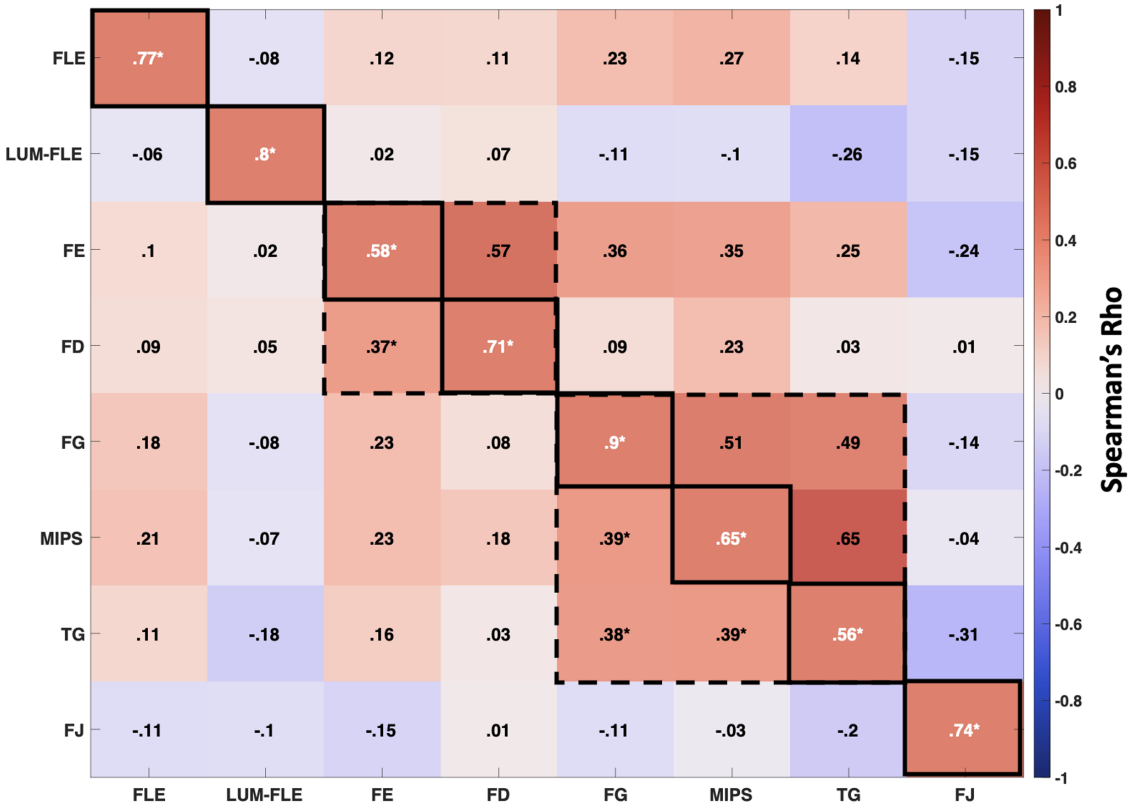

Figure 4. Spearman's rho correlations and test–retest reliability for the eight motion-position illusions. Diagonal solid black-bordered squares depict test–retest reliability across sessions for the respective illusion. The dashed black squares highlight the correlated clusters of illusions. Correlations below the diagonal represent the raw correlation values between illusions, and correlations above the diagonal represent disattenuated correlations. Asterisks represent significant correlations; *$p < 0.0018$ (Bonferroni-corrected alpha).

Sessions 1 and 2. Therefore, as shown in Table A4, we looked at correlations between the number of days between Sessions 1 and 2 and the difference in illusory effect from Sessions 1 to 2. There were no significant correlations observed via either Spearman's rho or Pearson's *R*. This suggests that the decrease in illusory effect from Sessions 1 to 2 may not be related to the number of days between sessions. However, we recommend that these results are interpreted cautiously, as we did not design this study with this analysis in mind and did not directly manipulate the number of days between sessions. As such, we may be underpowered to detect a true effect, and future studies should explore a wider range of temporal delays. The distribution of days between sessions is presented in Figure A1 and shows that 1, 6, and 7 days was the most frequent number of days between sessions.

Pairwise correlations

To investigate whether the different MPIs are likely to be the result of shared or dissociable mechanisms, Spearman's rho was calculated for illusion magnitudes for each pair of illusions (Figure 4). For completeness, Spearman's rho and Pearson's *R* are both presented in Table A5, alongside 95% confidence intervals. To correct the family-wise error rates for multiple comparisons, Bonferroni correction ($\alpha = 0.05/28$) was conducted. The *p* values for the correlation analyses are presented in Table A6. To control for participant factors that may be unique to a single session (e.g., mood, tiredness), we also investigated the Spearman's rho correlations between illusions across sessions (e.g., FLE Session 1 with FD Session 2; Goodbourn et al., 2012). These correlations and their *p* values are presented in Table A7. The first observation of note is that across most MPIs, illusion magnitudes did not correlate to a statistically significant degree. However, two clusters of statistically significant correlations emerged. The first cluster included significant positive correlations between the FG, TG, and the MIPS. All correlations were above 0.38, corresponding to moderate to large effects according to Cohen's (1988) guidelines or large effects according to Gignac and Szodorai's (2016) guidelines for interpreting correlations in individual differences research. The FE and FD were also significantly correlated, to a moderate

(Cohen, 1988) or large degree (Gignac & Szodorai, 2016).

Inspecting correlations between tasks across different sessions (e.g., correlating a participant's FE magnitude in Session 1 with their FD magnitude in Session 2), our results remain mostly unchanged (Table A7). The only change observed is that the MIPS no longer significantly correlates with the TG or FG (when p values are interpreted against the previously used Bonferroni-corrected alpha). This suggests that transient participant-related factors unique to a single session (e.g., tiredness) are unlikely to be a dominant factor driving these correlations.

The correlations discussed above represent estimates of the true effect size that are attenuated by possible measurement error (Hedge et al., 2018; Mollon et al., 2017; Spearman, 1987; Trafimow, 2016). Test–retest reliabilities provide an estimate of the noise of the measurement. To correct for this noise and calculate an estimate of the disattenuated ("true") correlation (Mollon et al., 2017), we calculated disattenuated ("true") Spearman's rhos (Figure 4) using Spearman's (1987) formula (Equation 1). In this equation, x and y represent separate illusions, and Reliability(x) and Reliability(y) refer to the test–retest reliability for the associated illusion.

$$\text{Disattentuated correlation } (x,\ y) = \frac{\textit{Pairwise correlation } (x,\ y)}{\sqrt{\textit{Reliability}\,(x) * \textit{Reliability}\,(y)}} \quad (1)$$

After disattenuation based on Equation 1, all four significant correlations identified above meet the criterion for "large effects" according to Gignac and Szodorai (2016) and Cohen (1988). However, note that while disattenuated correlations are estimates of the true correlation, they are not suitable for inference (Hedge et al., 2018). Disattenuated correlation coefficients are plotted above the diagonal in Figure 4. They show the same qualitative pattern of relationships between MPIs as the raw correlations.

Factor analysis

Having observed two main clusters of correlations with moderate to large effects, we further explored the underlying structure of these correlations using exploratory factor analysis.

An exploratory principal axis factor analysis with an oblique oblimin rotation was conducted using JASP 0.17.1 (JASP Team, 2023). The violation of normality for the distributions of illusion magnitude was not problematic, as this factor analysis seeks to describe the relationships between the illusions, not engage in statistical inference (Field, 2017; Tabachnick & Fidell, 2014). To verify the sampling adequacy for the analysis, the Kaiser–Meyer–Olkin (KMO) measure was explored and interpreted according to Kaiser and Rice's (1974) guidelines. The overall KMO (KMO = 0.630) was mediocre, and the FJ (KMO = 0.473) and LUM-FLE (KMO = 0.375) were unacceptable, with the remaining illusions having miserable to mediocre KMOs above 0.5 (Kaiser & Rice, 1974). Based on the low KMO value for the LUM-FLE, we removed it from the factor analysis. This increased the FJ's KMO (KMO = 0.489). The FJ's KMO was just on the border of miserable/unacceptable. When the analysis was repeated with FJ excluded, the interpretation remain unchanged. Therefore, we decided to retain the FJ in this analysis.

Illusion	Factor 1	Factor 2	Factor 3	Uniqueness
TG	**0.650**	−0.061	−0.149	0.534
FG	**0.632**	−0.014	0.004	0.606
MIPS	**0.629**	0.086	0.169	0.580
FD	−0.017	**0.764**	0.010	0.423
FE	0.185	**0.330**	−0.275	0.739
FJ	0.010	0.008	**0.601**	0.641
FLE	0.239	0.008	−0.121	0.916
LUM-FLE*	—	—	—	0.973

Table 1. Pattern matrix factor loadings after oblimin rotation. Missing cases excluded pairwise. Factor loadings above 0.32 are presented in bold. *Excluded from the final factor analysis.

To minimize data loss, the factor analysis was conducted with pairwise exclusion of missing values. Pairwise data exclusion includes all the participants not missing data for the two illusions being considered in each correlation (Kang, 2013). When the analysis was repeated with listwise exclusion, which excludes all participants with an estimate missing for any of the MPIs (Kang, 2013), the main interpretation was unchanged. Factor analysis with pairwise exclusion of missing values is reported below, and the factor analysis with listwise exclusion of missing values is provided in Table A8 and Figure A2. Using Kaiser's (1960) criterion, the rotated factor analysis identified three factors with an eigenvalue above 1 (Table 1). These three factors explained 36.6% of the total variance. Factor 1 explained 19.1% of the variance, Factor 2 explained 10.2%, and Factor 3 explained 7.3%. Inspection of the scree plot (Figure 5) indicated that only the first factor should be retained. To identify the MPIs that loaded on each factor, we followed Tabachnick and Fidell's (2014) recommendation, only interpreting variables with a factor loading above 0.32. A factor loading of 0.32 ensures we only interpret variables that account for at least 10% of the variance in a factor. The first factor comprised the same three MPIs that mutually correlated in our primary analysis: the FG, TG, and MIPS (and FD when repeated with listwise exclusion). The second factor comprised the FD and FE (FJ and TG when repeated with listwise exclusion), and

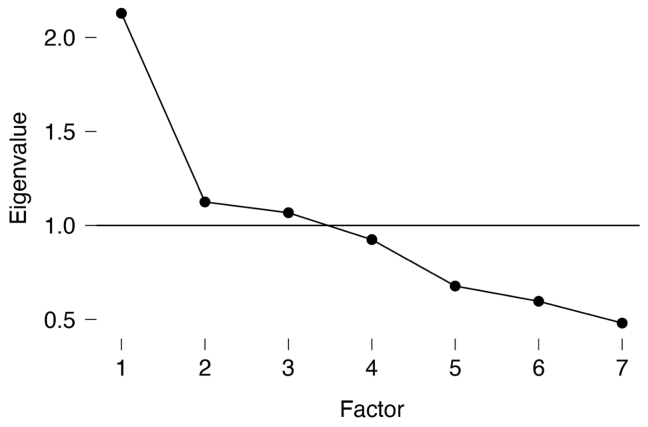

Figure 5. Exploratory factor analysis scree plot. The horizontal line at the y coordinate of 1 shows the eigenvalue criteria factors needed to exceed to be retained (Kaiser, 1960).

the third factor comprised the FJ (FE when repeated with listwise exclusion). Interestingly, regardless of the missing data exclusion rule used for the exploratory factor analysis, the FLE was the only illusion to not load on any factors. Table 1 displays the factor loadings for all illusions.

Overall, the exploratory factor analysis corroborated our correlation analyses, suggesting the FG, TG, and MIPS, as well as the FE and FD, share an underlying factor. More broadly, the limited loading of individual illusions on shared factors, the high uniqueness observed in the factor analysis, and the absence of further pairwise correlations suggest that other than these two correlated clusters, the different MPIs are likely to involve unique mechanisms.

Discussion

Motion-position illusions are a broad class of visual illusions in which motion signals cause the position of one or more objects to be misperceived. Although many of these illusions are phenomenologically similar, and many researchers have proposed individual theories designed to explain several of them, the degree to which they are the result of common underlying mechanisms is unknown. Here, we used a between-subjects correlational approach to investigate variations in illusion magnitude in eight MPIs: the flash-lag effect (FLE), the luminance flash-lag effect (LUM-FLE), the Fröhlich effect (FE), the flash-drag effect (FD), the flash-grab effect (FG), motion-induced position shift (MIPS), the twinkle-goes effect (TG), and the flash-jump effect (FJ).

We report three main results. First, there were three illusions for which individual differences in illusion magnitude were positively and statistically significantly intercorrelated: the FLE, MIPS, and TG. A subsequent exploratory factor analysis corroborated this pattern, finding that these three illusions loaded onto a single factor and thereby suggesting that they might share more underlying mechanisms with each other than with the other illusions. Second, we observed a positive correlation between the FE and FD, which was also corroborated by the exploratory factor analysis, showing these two illusions load onto a single factor and therefore supporting that these two illusions might also share a (different) common mechanism. Third, there is a common belief that many of these illusions are caused by a shared mechanism. It has been proposed that some of these illusions may be caused by motion biasing (Eagleman & Sejnowski, 2007), discrete subsampling (Schneider, 2018), motion extrapolation (Hogendoorn, 2020), and an interaction of global and local motion signals (Kwon et al., 2015). Contrary to this belief, we did not observe any other statistically significant correlations: Beyond the two shared factors identified, the factor analysis did not identify any other factors comprising more than one illusion. This suggests that the remaining MPIs may result from distinct, illusion-specific mechanisms.

We know that in order to perceive and judge the position of the stimuli, all the tasks must rely on some degree of shared neural mechanisms that are inherent to all visual perception tasks, such as the retina and early visual cortex (Goodbourn et al., 2012). It would be surprising if variation in such processes did not also cause (shared) variation in some of the present illusions. To speculate, the brains of those with lower visual acuity or motion sensitivity might rely more on their priors for speed or position than other participants, which could influence the magnitude of multiple several illusions in the current study. Indeed, we noted a range of small positive (nonsignificant) correlations across numerous MPI pairs that might reflect such shared variance, but it is notable that (if real) the correlation is evidently too subtle to be statistically significant with a study of this size.

Overall, our results reveal that MPIs are likely caused by both dissociable and shared mechanisms, because while there are two clusters of intercorrelated illusions, several illusions did not correlate with one another. Notably, despite the flash-lag effect being central to theoretical debates about the mechanisms underlying MPIs, and contrary to the typical assumption the FLE and other MPIs share an underlying cause (Eagleman & Sejnowski, 2007; Schneider, 2018), we observed only nonsignificant correlations of weak to moderate strength between the FLE and other illusions. This suggests that, beyond the low-level neural mechanisms common to all these illusions (e.g., retina and early visual cortex), some of these illusions arise from dissociable mechanisms. This is a surprising result and highlights the importance of us identifying the extent to

which these illusions are caused by common or distinct mechanisms.

In the MPI literature, there are unresolved debates regarding the similarities and differences of many illusions. By adopting an individual differences approach, we are able to address some of these debates. First, it has been argued that the FE and FLE may actually be the same phenomenon, since the FE has much in common with the flash-initiated FLE (Eagleman & Sejnowski, 2007). However, consistent with Morrow and Samaha (2022), our results suggest that these are separate illusions, as illusion magnitudes in the two paradigms were uncorrelated. Additionally, Eagleman and Sejnowski (2007) also argued that the FD and FLE are both caused by motion biasing and that they have inversely related effects, with the FD reducing as the FLE increases. If this were the case, we might expect a negative correlation between these two MPIs, but we observed no correlation at all, suggesting that they may in fact be unrelated. Third, Sheth et al. (2000) argued that different variants of the FLE in other feature spaces, including luminance (LUM-FLE), were caused by a shared domain-general mechanism. However, although we observed stable illusory effects for both the FLE and LUM-FLE, effect magnitudes were uncorrelated. This suggests that the FLE and LUM-FLE are caused by separate processes rather than a common process. Fourth, we also observed that the FG and FD effects were uncorrelated. This is consistent with the initial presentation of the FG by Cavanagh and Anstis (2013), who used the differences in their time course and attentional demands to argue that these were different phenomena. Finally, we found that the FLE and MIPS were not significantly correlated, which is consistent with a previous finding of a dissociation between them (Linares & Holcombe, 2008).

It is important to note that for each of the eight illusions we investigated, we observed strong illusion effects that were stable over time. As such, it seems unlikely that our results were overwhelmingly driven by noise or nonperceptual factors. If our estimates of illusion magnitudes were unduly affected by noise, this would have resulted in weak test–retest reliabilities, whereas our test–retest reliabilities were strong across all eight paradigms. Conversely, if correlations were caused by nonperceptual factors, such as experimenter expectancy bias or some kind of reporting bias, we would expect to observe correlations between all illusions, rather than between just two subsets (Hu et al., 2022). Therefore, it seems likely that our results accurately reflect the influence of dissociable underlying perceptual factors.

An additional incidental observation that we noted when inspecting illusion magnitudes across the two sessions is that all illusions had a small decrease in the mean illusory magnitude from Session 1 to Session 2 (Table A3). While this decrease in effect suggests that illusion magnitude is not stable over time, the strong test–retest reliabilities indicate that individual differences in the perception of MPIs remained stable over time (Cretenoud et al., 2021). These two observations are consistent with findings for geometric illusions (Cretenoud et al., 2021). Wexler et al. (2015) similarly showed that individual differences in the perception of motion stimuli stay stable for up to a year. If the effects of MPIs do decrease with time, practice, or exposure, this may make them different than at least some geometric illusions (Predebon, 2006). Further exploration of this finding and its implications is an interesting avenue for future research.

What features define the two subsets of illusions for which we observe significant associations? The main cluster of intercorrelated illusions includes the FG, TG, and MIPS. One shared feature of these three illusions is that they all involve position judgments about superimposed objects (in the FG, a disc is flashed on a moving annulus; in the TG, a dynamic noise background is presented when the target disappears; and in MIPS, participants judge the static envelope of a drifting texture). The same is not true for the remaining illusions. If spatial superposition is a defining feature connecting these illusions, then it seems likely that interactions between multiple, colocalized motion signals (e.g., local and global motion, or object and pattern motion) play a role in determining illusion magnitude (even when global motion signals have no net motion energy in any direction, as in dynamic noise background of the TG). This interpretation is supported by previous modeling work by Kwon et al. (2015). The second group of correlated illusions in our results includes the FE and FD. It is difficult to identify a single common feature of these two illusions that is not also shared by other MPIs. For instance, in both FE and FD, the position of a transient event (the object's own appearance, in the case of the FE) is shifted in the direction of subsequent motion. This likewise applies to the FG, yet FG only weakly correlated with the FE and had no correlation with the FD. Moreover, one might expect the FE to correlate with the flash-initiated FLE, which is identical in terms of presentation except for the presentation of a static flash. Although the flash-initiated FLE was not tested here, the flash-initiated FLE's illusion magnitudes are similar to the conventional FLE (Eagleman & Sejnowski, 2000). Therefore, we would expect the FLE and flash-initiated FLE to correlate with one another and be caused by a shared mechanism. In our data set, the FLE and FE did not correlate, suggesting that they may in fact be separate phenomena.

Overall, we observed strong correlations between two distinct groups of MPIs, with FG, TG, and MIPS making up one group and FD and FE making up the other. However, in both cases, it seems unlikely that the shared mechanism is the single underlying cause. Even

using the disattenuated correlations, pairs of illusions share only around 20–40% of the variance in illusion magnitude. Likewise, three factors identified in the exploratory factor analysis only explained 36.6% of the variance, with the primary shared factor (TG, FG, and MIPS) only explaining 19.1% of variance. Therefore, although there are clear, strong correlations between some illusions, the majority of the variance in each illusion is unaccounted for by its correlation with the other illusion(s). Consequently, it is likely that multiple different mechanisms contribute to each MPI. This interpretation is consistent with recent experimental and modeling evidence that showed a single theoretical account cannot explain the FG effect (Blom et al., 2019; Takao et al., 2022). It would therefore be valuable for future research to further tease apart the different mechanisms contributing to each of these illusions.

The general dissociation we observed between different MPIs argues against these illusions reflecting a single overarching neural process. One such process is motion extrapolation, which is a popular explanation for the FLE (Hogendoorn, 2020). Motion extrapolation refers to the use of previous information about an object's motion and trajectory to predict its future veridical position (Hogendoorn, 2020; Nijhawan, 2008). Motion extrapolation has been argued to be valuable in helping the brain overcome the neural delays inherent in communicating information throughout the nervous system (Hogendoorn, 2020; Nijhawan, 1994). Motion extrapolation has been observed to operate at multiple levels in the nervous system (Benvenuti et al., 2020; Berry et al., 1999; Blom et al., 2020; Hogendoorn & Burkitt, 2018; Jancke et al., 2004; Subramaniyan et al., 2018; van Heusden et al., 2019), and it has been argued to manifest perceptually as the FLE and related illusions. However, because motion extrapolation is argued to be an inherent process of the nervous system, if it was the predominant cause of the FLE, we would expect (a) all participants to experience a flash-lag effect (Holcombe, 2021) and (b) individual variability in motion extrapolation mechanisms to manifest as correlations in the resulting illusions. Contrary to this notion, the present study identified that some participants experienced stable effects in the direction opposite to the classical illusion effects (e.g., a flash-lead effect rather than a flash-lag effect or, to a lesser extent, a repulsion effect in the FD). This limitation applies to all popular MPI theories, none of which can explain why some individuals consistently experience the opposite of the usual effect for some illusions.

One neurophysiological variable that might act as a possible predictor of individual differences in MPIs is individual alpha frequency (IAF). IAF can be obtained from electroencephalographic recordings of participants while they complete eyes-open and eyes-closed resting state conditions (for more information on extracting IAF, see Corcoran et al., 2018). IAF has been positively correlated with and suggested to drive the temporal window of integration in the sound-induced double-flash illusion (Cecere et al., 2015), and faster alpha frequencies are related to greater flash discrimination accuracy on a two-flash fusion threshold task (Samaha & Postle, 2015). Therefore, exploring how IAF correlates with individual differences in MPIs is an interesting avenue for future research.

In designing the individual MPI paradigms, we aimed to stay close to the configuration in which each illusion was either first reported or most commonly presented. As a result, the different MPIs were presented at different eccentricities and positions in the visual field. Several studies have reported idiosyncratic differences in visual sensitivity and localization across different positions in the visual field (e.g., Barbot et al., 2021; Greenwood et al., 2017; Kosovicheva & Whitney, 2017), which may have reduced the association we observed between different illusions. However, for both of the clusters of correlating MPIs that we observed, the individual illusions correlate despite having widely divergent spatial configurations. For example, the FD involves vertically translating textures but correlates with the FE, which involves radial movement. Likewise, TG involves two horizontally translating objects that are compared near the vertical midline, MIPS involves horizontally drifting gratings in each of the four quadrants, and the FG involves rotating annular gratings and a flash directly below fixation. The fact that these MPIs correlate despite substantial configurational differences suggests that it is unlikely that idiosyncratic interindividual differences in visual sensitivity caused us to meaningfully underestimate true effects. Nevertheless, to minimize the possible impact of any such differences, it would be useful for future studies to adapt different MPI paradigms to match display configurations as closely as possible.

Beyond elucidating the factorial structure of MPIs, our results speak to the fundamental question of the multifactorial architecture of the human visual system. Over the past decade, researchers have wondered whether the multitude of visual functions might be subserved by a smaller number of common underlying processes. Based on the individual differences approach, the available evidence suggests that many visual phenomena, including geometric illusions (Cretenoud et al., 2019; Grzeczkowski et al., 2017, 2018), some motion paradigms (Hu et al., 2022; Wexler et al., 2022), four magnocellular tasks (Goodbourn et al., 2012), binocular rivalry (Brascamp et al., 2019), simultaneous contrast (Bosten & Mollon, 2010), and performance on a range of visual psychophysical tests (Cappe et al., 2014; Shaqiri et al., 2019; Ward et al., 2017), are unlikely to be caused by a single common factor or process but instead reflect multiple factors. Our finding that MPIs are not caused by a single shared factor extends this

research and supports the emerging perspective that there is no general common factor in vision (Cappe et al., 2014; Tulver, 2019).

In sum, the present study used an individual differences approach to investigate the factorial structure of eight motion-position illusions. We observed two separate groups of intercorrelated illusions but no evidence for broader shared mechanisms. This demonstrates that despite the phenomenological similarity of illusions in this class, and contrary to the prevailing, if implicit, view in the field, different illusions are likely to result from different mechanisms. Furthermore, we found evidence that rather than resulting from a single mechanism, individual illusions likely result from an interplay of different mechanisms. Further research is needed to unravel the contribution of different mechanisms to illusions in this class and more broadly how they interact to influence the localization of objects in our dynamic visual world.

Keywords: individual differences, flash-lag effect, Fröhlich effect, flash-drag effect, flash-grab effect, motion-induced position shift, twinkle-goes effect, flash-jump effect, shared mechanisms

Acknowledgments

The authors thank the Timing in Brain and Behaviour Laboratory for the helpful discussion and support over the past few years.

TC was supported by an Australian Government Research Training Program Stipend (RTP). HH acknowledges funding from the Australian Research Council (DP180102268 and FT200100246).

Commercial relationships: none.
Corresponding author: Timothy V. Cottier.
Email: tcottier@student.unimelb.edu.au.
Address: Melbourne School of Psychological Sciences, the University of Melbourne, Melbourne, Australia.

References

Allen, M., Poggiali, D., Whitaker, K., Marshall, T. R., & Kievit, R. A. (2019). Raincloud plots: A multi-platform tool for robust data visualization [version 1; peer review: 2 approved]. *Wellcome Open Research, 4*, 1–51, https://doi.org/10.12688/wellcomeopenres.15191.1.

Anstis, S. (1989). Kinetic edges become displaced, segregated, and invisible. *Neural Mechanisms of Visual Perception, 2*, 247–260.

Baldo, M. V. C., & Klein, S. A. (1995). Extrapolation or attention shift? *Nature, 378*(6557), 565–566, https://doi.org/10.1038/378565a0.

Barbot, A., Xue, S., & Carrasco, M. (2021). Asymmetries in visual acuity around the visual field. *Journal of Vision, 21*(1), 1–23, https://doi.org/10.1167/jov.21.1.2.

Benvenuti, G., Chemla, S., Boonman, A., Perrinet, L., Masson, G., & Chavane, F. (2020). Anticipatory responses along motion trajectories in awake monkey area V1. *BioRxiv,* https://doi.org/10.1101/2020.03.26.010017.

Berry, M. J., Brivanlou, I. H., Jordan, T. A., & Meister, Markus. (1999). Anticipation of moving stimuli by the retina. *Nature, 398*, 334–338, https://doi.org/10.1038/18678.

Blom, T., Feuerriegel, D., Johnson, P., Bode, S., & Hogendoorn, H. (2020). Predictions drive neural representations of visual events ahead of incoming sensory information. *Proceedings of the National Academy of Sciences, 117*(13), 7510–7515, https://doi.org/10.1073/pnas.1917777117.

Blom, T., Liang, Q., & Hogendoorn, H. (2019). When predictions fail: Correction for extrapolation in the flash-grab effect. *Journal of Vision, 19*(2), 1–11, https://doi.org/10.1167/19.2.3.

Bosten, J. M., & Mollon, J. D. (2010). Is there a general trait of susceptibility to simultaneous contrast? *Vision Research, 50*(17), 1656–1664, https://doi.org/10.1016/j.visres.2010.05.012.

Brascamp, J. W., Qian, C. S., Hambrick, D. Z., & Becker, M. W. (2019). Individual differences point to two separate processes involved in the resolution of binocular rivalry. *Journal of Vision, 19*(12), 15, https://doi.org/10.1167/19.12.15.

Cai, R., & Schlag, J. (2001). A new form of illusory conjunction between color and shape. *Journal of Vision, 1*(3), 127, https://doi.org/10.1167/1.3.127.

Cambridge Research Systems. (2018). ColorCAL MKII Colorimeter [Computer software], https://www.crsltd.com/tools-for-vision-science/light-measurement-display-calibation/colorcal-mkii-colorimeter/.

Cappe, C., Clarke, A., Mohr, C., & Herzog, M. H. (2014). Is there a common factor for vision? Cappe. *Journal of Vision, 14*(8), 1–11, https://doi.org/10.1167/14.8.4.

Cavanagh, P., & Anstis, S. (2013). The flash grab effect. *Vision Research, 91*, 8–20, https://doi.org/10.1016/j.visres.2013.07.007.

Cecere, R., Rees, G., & Romei, V. (2015). Individual differences in alpha frequency drive crossmodal illusory perception. *Current Biology, 25*(2), 231–235, https://doi.org/10.1016/j.cub.2014.11.034.

Clark, K., Birch-Hurst, K., Pennington, C. R., Petrie, A. C. P., Lee, J. T., & Hedge, C. (2022). Test-retest reliability for common tasks in vision science. *Journal of Vision, 22*(8), 18, https://doi.org/10.1167/jov.22.8.18.

Cohen, J. (1988). *Statistical power analysis for the behavioral sciences* (2nd ed.). New York: Routledge, https://doi.org/10.4324/9780203771587.

Corcoran, A. W., Alday, P. M., Schlesewsky, M., & Bornkessel-Schlesewsky, I. (2018). Toward a reliable, automated method of individual alpha frequency (IAF) quantification. *Psychophysiology, 55*(7), 1–21, https://doi.org/10.1111/psyp.13064.

Cretenoud, A. F., Grzeczkowski, L., Kunchulia, M., & Herzog, M. H. (2021). Individual differences in the perception of visual illusions are stable across different contexts. *Journal of Vision, 21*(5), 26, https://doi.org/10.1167/jov.21.5.26.

Cretenoud, A. F., Karimpur, H., Grzeczkowski, L., Francis, G., Hamburger, K., & Herzog, M. H. (2019). Factors underlying visual illusions are illusion-specific but not feature-specific. *Journal of Vision, 19*(14), 1–21, https://doi.org/10.1167/19.14.12.

De Valois, R. L., & De Valois, K. K. (1991). Vernier acuity with stationary moving Gabors. *Vision Research, 31*(9), 1619–1626, https://doi.org/10.1016/0042-6989(91)90138-U.

Eagleman, D. M., & Sejnowski, T. J. (2000). Motion integration and postdiction in visual awareness. *Science, 287*(5460), 2036–2038, https://doi.org/10.1126/science.287.5460.2036.

Eagleman, D. M., & Sejnowski, T. J. (2007). Motion signals bias localization judgments: A unified explanation for the flash-lag, flash-drag, flash-jump, and Frohlich illusions. *Journal of Vision, 7*(4), 1–12, https://doi.org/10.1167/7.4.3.

Efron, B., & Tibshriani, R. J. (1994). *An introduction to the bootstrap*. New York: Chapman and Hall/CRC, https://www.taylorfrancis.com/books/mono/10.1201/9780429246593/introduction-bootstrap-bradley-efron-tibshirani.

Field, A. (2017). *Discovering statistics using IBM SPSS statistics* (5th ed.). Thousand Oaks, CA: SAGE.

Fröhlich, F. (1924). Über die messung der empfindungszeit. *Pflüger's Archiv Für Die Gesamte Physiologie Des Menschen Und Der Tiere, 202*, 566–572, https://doi.org/10.1007/BF01723521.

Gauch, A., & Kerzel, D. (2008). Comparison of flashed and moving probes in the flash-lag effect: Evidence for misbinding of abrupt and continuous changes. *Vision Research, 48*(15), 1584–1591, https://doi.org/10.1016/j.visres.2008.04.025.

Gignac, G. E., & Szodorai, E. T. (2016). Effect size guidelines for individual differences researchers. *Personality and Individual Differences, 102*, 74–78, https://doi.org/10.1016/j.paid.2016.06.069.

Goodbourn, P. T., Bosten, J. M., Hogg, R. E., Bargary, G., Lawrance-Owen, A. J., & Mollon, J. D. (2012). Do different "magnocellular tasks" probe the same neural substrate? *Proceedings of the Royal Society B: Biological Sciences, 279*(1745), 4263–4271, https://doi.org/10.1098/rspb.2012.1430.

Greenwood, J. A., Szinte, M., Sayim, B., & Cavanagh, P. (2017). Variations in crowding, saccadic precision, and spatial localization reveal the shared topology of spatial vision. *Proceedings of the National Academy of Sciences, 114*(17), E3573–E3582, https://doi.org/10.1073/pnas.1615504114.

Grzeczkowski, L., Clarke, A. M., Francis, G., Mast, F. W., & Herzog, M. H. (2017). About individual differences in vision. *Vision Research, 141*, 282–292, https://doi.org/10.1016/j.visres.2016.10.006.

Grzeczkowski, L., Roinishvili, M., Chkonia, E., Brand, A., Mast, F. W., Herzog, M. H., . . . Shaqiri, A. (2018). Is the perception of illusions abnormal in schizophrenia? *Psychiatry Research, 270*, 929–939, https://doi.org/10.1016/j.psychres.2018.10.063.

Hedge, C., Powell, G., & Sumner, P. (2018). The reliability paradox: Why robust cognitive tasks do not produce reliable individual differences. *Behavior Research Methods, 50*(3), 1166–1186, https://doi.org/10.3758/s13428-017-0935-1.

Hogendoorn, H. (2020). Motion extrapolation in visual processing: Lessons from 25 years of flash-lag debate. *Journal of Neuroscience, 40*(30), 5698–5705, https://doi.org/10.1523/JNEUROSCI.0275-20.2020.

Hogendoorn, H., & Burkitt, A. N. (2018). Predictive coding of visual object position ahead of moving objects revealed by time-resolved EEG decoding. *NeuroImage, 171*, 55–61, https://doi.org/10.1016/j.neuroimage.2017.12.063.

Hogendoorn, H., Verstraten, F. A. J., & Cavanagh, P. (2015). Strikingly rapid neural basis of motion-induced position shifts revealed by high temporal-resolution EEG pattern classification. *Vision Research, 113*(Pt. A), 1–10, https://doi.org/10.1016/j.visres.2015.05.005.

Holcombe, A. O. (2021). When average is over: Small N but many trials. *Journal of Cognition, 4*(1), 47, https://doi.org/10.5334/joc.168.

Hu, D., Ison, M., & Johnston, A. (2022). Exploring the common mechanisms of motion-based visual prediction. *Frontiers in Psychology, 13*, 1–12, https://doi.org/10.3389/fpsyg.2022.827029.

Hubbard, T. L. (2014). The flash-lag effect and related mislocalizations: Findings, properties, and theories. *Psychological Bulletin, 140*(1), 308–338, https://doi.org/10.1037/a0032899.

Jancke, D., Erlhagen, W., Schöner, G., & Dinse, H. R. (2004). Shorter latencies for motion trajectories than for flashes in population responses of cat primary visual cortex. *The Journal of Physiology, 556*(3), 971–982, https://doi.org/10.1113/jphysiol.2003.058941.

JASP Team. (2023). JASP (Version 0.17.1) [Computer software], https://jasp-stats.org.

Kaiser, H. F. (1960). The application of electronic computers to factor analysis. *Educational and Psychological Measurement, 20*(1), 141–151, https://doi.org/10.1177/001316446002000116.

Kaiser, H. F., & Rice, J. (1974). Little Jiffy, Mark Iv. *Educational and Psychological Measurement, 34*, 111–117, https://doi.org/10.1177/001316447403400115.

Kang, H. (2013). The prevention and handling of the missing data. *Korean Journal of Anesthesiology, 64*(5), 402–406, https://doi.org/10.4097/kjae.2013.64.5.402.

Kosovicheva, A., & Whitney, D. (2017). Stable individual signatures in object localization. *Current Biology, 27*(14), 1–5, https://doi.org/10.1016/j.cub.2017.06.001.

Krekelberg, B., & Lappe, M. (2000). A model of the perceived relative positions of moving objects based upon a slow averaging process. *Vision Research, 40*(2), 201–215, https://doi.org/10.1016/S0042-6989(99)00168-6.

Krekelberg, B., & Lappe, M. (2001). Neuronal latencies and the position of moving objects. *Trends in Neurosciences, 24*(6), 335–339, https://doi.org/10.1016/S0166-2236(00)01795-1.

Kwon, O., Tadin, D., & Knill, D. C. (2015). Unifying account of visual motion and position perception. *Proceedings of the National Academy of Sciences of the United States of America, 112*(26), 8142–8147, https://doi.org/10.1073/pnas.1500361112.

Linares, D., & Holcombe, A. O. (2008). Position perception: Influence of motion with displacement dissociated from the influence of motion alone. *Journal of Neurophysiology, 100*(5), 2472–2476, https://doi.org/10.1152/jn.90682.2008.

Mackay, D. M. (1958). Perceptual stability of a stroboscopically lit visual field containing self-luminous objects. *Nature, 181*(4607), 507–508, https://doi.org/10.1038/181507a0.

Maus, G. W., & Nijhawan, R. (2006). Forward displacements of fading objects in motion: The role of transient signals in perceiving position. *Vision Research, 46*(26), 4375–4381, https://doi.org/10.1016/j.visres.2006.08.028.

Maus, G. W., & Nijhawan, R. (2008). Motion extrapolation into the blind spot. *Psychological Science, 19*(11), 1087–1091, https://doi.org/10.1111/j.1467-9280.2008.02205.x.

Metzger, W. (1932). Versuch einer gemeinsamen Theorie der Phänomene Fröhlichs und Hazelhoffs und Kritik ihrer Verfahren zur Messung der Empfindungszeit. *Psychologische Forschung Volume, 16*, 176–200.

Microsoft. (2018). Windows 10 Pro (Version 1803) [Computer software], https://www.microsoft.com/en-au/d/windows-10-pro/df77x4d43rkt?activetab=pivot:overviewtab.

Mollon, J. D., Bosten, J. M., Peterzell, D. H., & Webster, M. A. (2017). Individual differences in visual science: What can be learned and what is good experimental practice? *Vision Research, 141*, 4–15, https://doi.org/10.1016/j.visres.2017.11.001.

Morrow, A., & Samaha, J. (2022). No evidence for a single oscillator underlying discrete visual percepts. *The European Journal of Neuroscience, 55*(11–12), 1–23, https://doi.org/10.1111/ejn.15362.

Nakayama, R., & Holcombe, A. O. (2021). A dynamic noise background reveals perceptual motion extrapolation: The twinkle-goes illusion. *Journal of Vision, 21*(11), 14, https://doi.org/10.1167/jov.21.11.14.

Nijhawan, R. (1994). Motion extrapolation in catching. *Nature, 370*, 256–257, https://doi.org/10.1038/370256b0.

Nijhawan, R. (2008). Visual prediction: Psychophysics and neurophysiology of compensation for time delays. *Behavioral and Brain Sciences, 31*(2), 179–239, https://doi.org/10.1017/S0140525X08003804.

Peirce, J. W., Gray, J. R., Simpson, S., MacAskill, M. R., Höchenberger, R., Sogo, H., . . . Lindeløv, J. (2019). PsychoPy2: Experiments in behavior made easy. *Behavior Research Methods, 51*, 195–203, https://doi.org/10.3758/s13428-018-01193-y.

Peirce, J. W., Hirst, R. J., & MacAskill, M. R. (2022). *Building experiments in PsychoPy* (2nd ed.). Los Angeles, CA: SAGE.

Predebon, J. (2006). Decrement of the Müller-Lyer and Poggendorff illusions: The effects of inspection and practice. *Psychological Research, 70*, 384–394, https://doi.org/10.1007/s00426-005-0229-6.

Ramachandran, V. S., & Anstis, S. M. (1990). Illusory displacement of equiluminous

kinetic edges. *Perception, 19*(5), 611–616, https://doi.org/10.1068/p190611.

Samaha, J., & Postle, B. R. (2015). The speed of alpha-band oscillations predicts the temporal resolution of visual perception. *Current Biology, 25*(22), 2985–2990, https://doi.org/10.1016/j.cub.2015.10.007.

Schneider, K. A. (2018). The flash-lag, Fröhlich and related motion illusions are natural consequences of discrete sampling in the visual system. *Frontiers in Psychology, 9*(1227), 1–8, https://doi.org/10.3389/fpsyg.2018.01227.

Schwarzkopf, D. S., Song, C., & Rees, G. (2011). The surface area of human V1 predicts the subjective experience of object size. *Nature Neuroscience, 14*(1), 28–30, https://doi.org/10.1038/nn.2706.

Shaqiri, A., Pilz, K. S., Cretenoud, A. F., Neumann, K., Clarke, A., Kunchulia, M., … Herzog, M. H. (2019). No evidence for a common factor underlying visual abilities in healthy older people. *Developmental Psychology, 55*(8), 1775–1787, https://doi.org/10.1037/dev0000740.

Sheth, B. R., Nijhawan, R., & Shimojo, S. (2000). Changing objects lead briefly flashed ones. *Nature Neuroscience, 3*(5), 489–495, https://doi.org/10.1038/74865.

Shi, Z., & Nijhawan, R. (2012). Motion extrapolation in the central fovea. *PLoS ONE, 7*(3), 33651, https://doi.org/10.1371/journal.pone.0033651.

Spearman, C. (1987). The proof and measurement of association between two things. *The American Journal of Psychology, 100*(3/4), 441–471, https://doi.org/10.2307/1422689.

Subramaniyan, M., Ecker, A. S., Patel, S. S., Cotton, R. J., Bethge, M., Pitkow, X., … Tolias, A. S. (2018). Faster processing of moving compared with flashed bars in awake macaque V1 provides a neural correlate of the flash lag illusion. *Journal of Neurophysiology, 120*(5), 2430–2452, https://doi.org/10.1152/jn.00792.2017.

Tabachnick, B., & Fidell, L. (2014). *Using multivariate statistics* (6th ed.). Harlow, Essex: Pearson Education.

Takao, S., Sarodo, A., Anstis, S., Watanabe, K., & Cavanagh, P. (2022). A motion-induced position shift that depends on motion both before and after the test probe. *Journal of Vision, 22*(12), 19, https://doi.org/10.1167/jov.22.12.19.

The MathWorks Inc. (2021). MATLAB (Version 9.11 (R2021B)) [Computer software], https://www.mathworks.com.

Trafimow, D. (2016). The attenuation of correlation coefficients: A statistical literacy issue. *Teaching Statistics, 38*(1), 25–28, https://doi.org/10.1111/test.12087.

Tulver, K. (2019). The factorial structure of individual differences in visual perception. *Consciousness and Cognition, 73*, 1–8, https://doi.org/10.1016/j.concog.2019.102762.

van Heusden, E., Harris, A. M., Garrido, M. I., & Hogendoorn, H. (2019). Predictive coding of visual motion in both monocular and binocular human visual processing. *Journal of Vision, 19*(1), 1–12, https://doi.org/10.1167/19.1.3.

Ward, J., Rothen, N., Chang, A., & Kanai, R. (2017). The structure of inter-individual differences in visual ability: Evidence from the general population and synaesthesia. *Vision Research, 141*, 293–302, https://doi.org/10.1016/j.visres.2016.06.009.

Wexler, M., Duyck, M., & Mamassian, P. (2015). Persistent states in vision break universality and time invariance. *Proceedings of the National Academy of Sciences, 112*(48), 14990–14995, https://doi.org/10.1073/pnas.1508847112.

Wexler, M., Mamassian, P., & Schütz, A. C. (2022). Structure of visual biases revealed by individual differences. *Vision Research, 195*(108014), 1–11, https://doi.org/10.1016/j.visres.2022.108014.

Whitney, D., & Cavanagh, P. (2000). Motion distorts visual space: Shifting the perceived position of remote stationary objects. *Nature Neuroscience, 3*, 954–959, https://doi.org/10.1038/78878.

Whitney, D., & Murakami, I. (1998). Latency difference, not spatial extrapolation. *Nature Neuroscience, 1*(8), 656–657, https://doi.org/10.1038/3659.

Whitney, D., Murakami, I., & Cavanagh, P. (2000). Illusory spatial offset of a flash relative to a moving stimulus is caused by differential latencies for moving and flashed stimuli. *Vision Research, 40*(2), 137–149, https://doi.org/10.1016/S0042-6989(99)00166-2.

Appendix

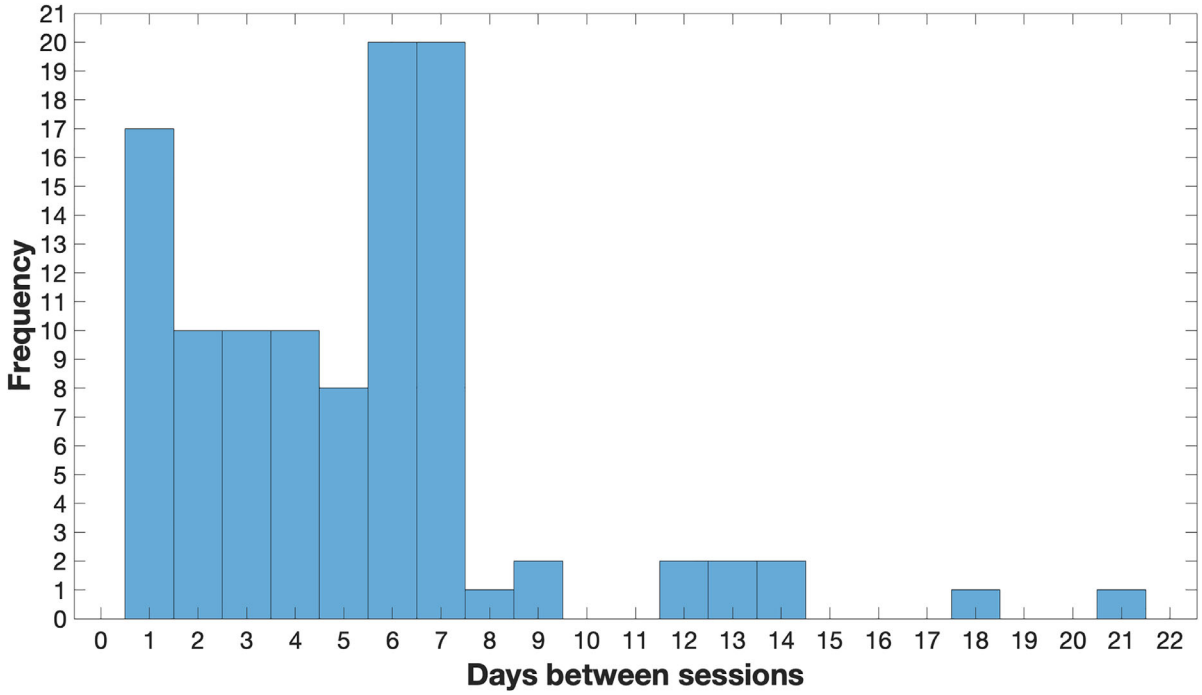

Figure A1. A histogram of the frequency (y-axis) of the number of days between sessions (x-axis).

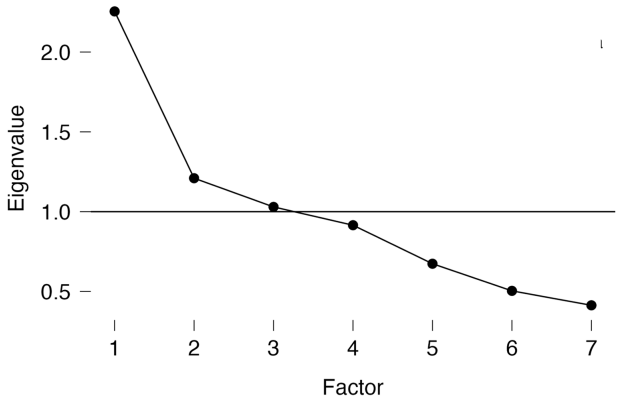

Figure A2. Exploratory factor analysis scree plot. Missing cases excluded listwise. Consistent with the scree plot when missing cases were excluded pairwise, the listwise scree plot suggests there is only one notable factor underlying the eight MPIs.

	Kolmogorov–Smirnov statistic (*df*)		
Illusion	Session 1	Session 2	Average effect
Flash-lag effect (FLE)	$D\,(84) = 0.54$	$D\,(84) = 0.43$	$D\,(84) = 0.51$
Flash-lag luminance effect (LUM-FLE)	$D\,(82) = 0.44$	$D\,(82) = 0.46$	$D\,(82) = 0.45$
Fröhlich effect (FE)	$D\,(81) = 0.43$	$D\,(81) = 0.40$	$D\,(81) = 0.40$
Flash-drag effect (FD)	$D\,(102) = 0.46$	$D\,(102) = 0.45$	$D\,(102) = 0.46$
Flash-grab effect (FG)	$D\,(98) = 0.95$	$D\,(98) = 0.93$	$D\,(98) = 0.94$
Motion-induced position shift (MIPS)	$D\,(103) = 0.64$	$D\,(103) = 0.59$	$D\,(103) = 0.62$
Twinkle-goes (TG)	$D\,(95) = 0.48$	$D\,(95) = 0.47$	$D\,(95) = 0.49$
Flash-jump (FJ)	$D\,(96) = 0.40$	$D\,(96) = 0.35$	$D\,(96) = 0.37$

Table A1. Kolmogorov–Smirnov tests for each illusion. All Kolmogorov–Smirnov tests were significant ($p < 0.001$).

Illusion (*N*)	Pearson's *R*
Flash-lag (85)	0.75
Luminance flash-lag (83)	0.76
Fröhlich (82)	0.54
Flash-drag (103)	0.75
Flash-grab (99)	0.89
Motion-induced position shift (104)	0.74
Twinkle-goes (96)	0.57
Flash-jump (97)	0.72

Table A2. Pearson's correlations values for the correlation between Sessions 1 and 2 for each illusion. N = sample size. All correlations significant $p < 0.01$.

	M (SD)		
Illusion	Session 1	Session 2	Average effect
Flash-lag effect (FLE)	2.02 (1.94)	1.37 (1.87)	1.70 (1.78)
Luminance flash-lag effect (LUM-FLE)	11 (14)	13 (13)	12 (13)
Fröhlich effect (FE)	1.32 (1.64)	1.08 (1.45)	1.2 (1.36)
Flash-drag effect (FD)	0.07 (0.08)	0.05 (0.07)	0.06 (0.07)
Flash-grab effect (FG)	4.52 (1.71)	4.15 (1.68)	4.34 (1.65)
Motion-induced position shift (MIPS)	0.81 (0.29)	0.65 (0.24)	0.73 (0.25)
Twinkle-goes effect (TG)	0.42 (0.35)	0.35 (0.24)	0.38 (0.26)
Flash-jump effect (FJ)	0.49 (0.45)	0.39 (0.42)	0.44 (0.40)

Table A3. Mean effect and standard deviation for each illusion's magnitude. All effects but LUM-FLE are in the degrees of visual angle (dva). LUM-FLE's effect is in luminance contrast (%).

Illusion	Spearman's rho (*p*)	Pearson's *r* (*p*)
Flash-lag effect (FLE)	0.163 (0.137)	0.040 (0.717)
Luminance flash-lag effect (LUM-FLE)	0.088 (0.428)	−0.014 (0.899)
Fröhlich effect (FE)	0.154 (0.151)	0.149 (0.165)
Flash-drag effect (FD)	0.05 (0.615)	0.109 (0.272)
Flash-grab effect (FG)	−0.064 (0.531)	−0.011 (0.911)
Motion-induced position shift (MIPS)	−0.106 (0.286)	−0.097 (0.328)
Twinkle-goes effect (TG)	0.052 (0.612)	0.072 (0.486)
Flash-jump effect (FJ)	−0.125 (0.221)	−0.122 (0.236)

Table A4. Spearman's rho and Pearson's *r* correlations between the number of days between sessions and the difference in illusory effect from Sessions 1 to 2.

illusion	FLE	LUM-FLE	FE	FD	FG	MIPS	TG	FJ
FLE		0.009 [-0.221, 0.259]	0.092 [-0.155, 0.290]	0.047 [-0.235, 0.321]	0.253 [-0.008, 0.459]	0.154 [-0.083, 0.349]	0.106 [-0.157, 0.326]	-0.133 [-0.324, 0.102]
LUM-FLE	-0.064 [-0.312, 0.205]		0.035 [-0.230, 0.265]	-0.003 [-0.230, 0.208]	0.016 [-0.237, 0.277]	- 0.028 [-0.252, 0.188]	-0.092 [-0.292, 0.118]	-0.112 [-0.336, 0.107]
FE	0.098 [-0.144, 0.336]	0.016 [-0.243, 0.263]		0.274 [0.060, 0.460]	0.192 [-0.047, 0.414]	0.163 [-0.025, 0.372]	0.272 [0.051, 0.543]	-0.158 [-0.400, 0.102]
FD	0.088 [-0.148, 0.316]	0.049 [-0.169, 0.266]	0.370 [0.161, 0.555]		0.110 [-0.055, 0.323]	0.201 [0.010, 0.384]	0.045 [-0.160, 0.247]	0.035 [-0.177, 0.275]
FG	0.180 [-0.057, 0.403]	-0.076 [-0.297, 0.148]	0.232 [-0.009, 0.428]	0.076 [-0.111, 0.254]		0.363 [0.150, 0.515]	0.411 [0.229, 0.578]	-0.046 [-0.245, 0.141]
MIPS	0.220 [-0.027, 0.435]	-0.071 [-0.303, 0.144]	0.225 [-0.016, 0.430]	0.181 [-0.018, 0.363]	0.392 [0.196, 0.546]		0.406 [0.224, 0.579]	0.035 [-0.169, 0.264]
TG	0.112 [-0.119, 0.330]	-0.178 [-0.400, 0.033]	0.160 [-0.073, 0.367]	0.027 [-0.213, 0.238]	0.375 [0.196, 0.546]	0.390 [0.185, 0.558]		-0.168 [-0.33, 0.036]
FJ	-0.115 [-0.320, 0.127]	-0.099 [-0.322, 0.117]	-0.155 [-0.381, 0.088]	0.007 [-0.226, 0.233]	-0.110 [-0.309, 0.072]	-0.025 [-0.206, 0.195]	-0.199 [-0.396, 0.010]	

Table A5. Pairwise correlation analyses between the average effect for each illusion. The black diagonal line separates Spearman's rho and Pearson's *r*. Spearman's rho values are presented on the bottom left of the diagonal line (blue), and Pearson's *r* is presented on the top right of the diagonal line (orange). The 95% bias-corrected and accelerated bootstrapped confidence intervals are in square brackets ($N = 1{,}000$). The precise significance values are provided in Table A6.

Illusion	FLE	LUM-FLE	FE	FD	FG	MIPS	TG
LUM-FLE	0.606						
FE	0.419	0.901					
FD	0.431	0.663	**				
FG	0.104	0.505	0.038	0.460			
MIPS	0.055	0.528	0.042	0.070	**		
TG	0.318	0.120	0.162	0.799	**	**	
FJ	0.310	0.388	0.176	0.949	0.295	0.808	0.575

Table A6. *P* values for each pairwise correlation $^{**}p < 0.001$. Correlation analyses are Spearman's rho. The *p* values are not corrected for multiple comparisons.

		Session 2							
	Illusion	FLE	LUM-FLE	FE	FD	FG	MIPS	TG	FJ
Session 1	FLE	0.768*	−0.044 (0.719)	0.071 (0.562)	0.037 (0.741)	0.188 (0.089)	0.156 (0.159)	0.09 (0.427)	−0.065 (0.567)
	LUM-FLE	−0.06 (0.627)	0.803*	−0.028 (0.821)	0.101 (0.371)	−0.103 (0.367)	0.02 (0.861)	−0.192 (0.094)	−0.035 (0.764)
	FE	0.137 (0.258)	0.084 (0.505)	0.582*	0.302 (0.006)	0.164 (0.145)	0.277 (0.012)	0.197 (0.084)	−0.141 (0.217)
	FD	0.1 (0.371)	0.008 (0.943)	0.388*	0.715*	0.201 (0.048)	0.162 (0.106)	0.032 (0.757)	−0.012 (0.91)
	FG	0.118 (0.29)	−0.013 (0.911)	0.296 (0.008)	−0.045 (0.665)	0.899*	0.379*	0.338 (0.001)	−0.121 (0.246)
	MIPS	0.221 (0.045)	−0.158 (0.16)	0.121 (0.281)	0.201 (0.044)	0.306 (0.002)	0.651*	0.274 (0.008)	−0.013 (0.9)
	TG	0.153 (0.173)	−0.005 (0.963)	0.113 (0.326)	0.057 (0.588)	0.343*	0.365*	0.557*	−0.143 (0.175)
	FJ	−0.158 (0.162)	−0.109 (0.346)	−0.083 (0.468)	0.03 (0.776)	−0.05 (0.634)	−0.068 (0.509)	−0.135 (0.2)	0.74*

Table A7. Correlations between illusions, Sessions 1 and 2, and Sessions 2 and 1. The *p* values are presented in brackets. $^{*}p < 0.001$. Gray cells show correlations with $p < 0.0018$ (Bonferroni-corrected alpha used in the main correlation analyses).

Illusion	Factor 1	Factor 2	Factor 3	Uniqueness
FG	**0.735**	0.029	−0.070	0.483
MIPS	**0.688**	0.079	0.063	0.508
TG	**0.508**	**−0.367**	0.028	0.559
FD	**0.366**	0.075	0.287	0.738
FJ	0.027	**0.882**	−0.008	0.224
FE	−0.016	−0.011	**0.771**	0.409
FLE	0.209	−0.131	0.044	0.926
LUM-FLE*	—	—	—	0.976

Table A8. Factor loading of the principal axis factor analysis following oblique oblimin rotation with missing cases excluded listwise. Pattern matrix factor loadings with missing cases excluded listwise. Factor loadings above 0.32 are in bold. *LUM-FLE was removed from the factor analysis due to a low KMO.